Molecular Therapy
Nucleic Acids
Original Article

lncRNA HIF1A Antisense RNA 2 Modulates Trophoblast Cell Invasion and Proliferation through Upregulating PHLDA1 Expression

Dan Wu,[1,2,6] Nana Yang,[1,6] Yetao Xu,[1,6] Sailan Wang,[1] Yuanyuan Zhang,[1] Matthew Sagnelli,[3] Bingqing Hui,[4] Zhenyao Huang,[5] and Lizhou Sun[1]

[1]Department of Obstetrics and Gynecology, First Affiliated Hospital of Nanjing Medical University, Nanjing 210029, Jiangsu Province, China; [2]Department of Neurobiology, Care Science and Society, Karolinska Institutet, Solna 17177, Sweden; [3]University of Connecticut School of Medicine, Farmington, CT 06030, USA; [4]Department of Oncology, Second Affiliated Hospital of Nanjing Medical University, Nanjing 210000, Jiangsu Province, China; [5]Key Laboratory of Modern Toxicology of Ministry of Education, School of Public Health, Nanjing Medical University, Nanjing 210029, Jiangsu Province, China

Long noncoding RNAs (lncRNAs) have been reported to be involved in various human diseases, and increasing studies have revealed that lncRNAs can play a vital role in preeclampsia (PE). In our study, lncRNA hypoxia-inducible factor 1 alpha (HIF1A) antisense RNA 2 (HIF1A-AS2) was found to be significantly downregulated in placenta tissues of PE patients by quantitative real-time PCR analysis. Moreover, Cell Counting Kit-8 (CCK-8) assays showed that downregulation of HIF1A-AS2 can impede cell proliferation of HTR-8/SVneo and JAR trophoblasts cells. Ectopic overexpression of HIF1A-AS2 can increase the function of trophoblasts cell migration and invasion *in vitro*. RNA-sequencing (RNA-seq), RNA immunoprecipitation (RIP), and chromatin immunoprecipitation (ChIP) experiments showed that HIF1A-AS2 can recruit lysine-specific demethylase 1 (LSD1) and epigenetically repress pleckstrin homology-like domain, family A, member 1 (PHLDA1) transcription in human trophoblasts cells. In summary, our findings suggest that downregulated HIF1A-AS2 may play a role in the pathogenesis and progression of PE, and has potential as a novel prognostic marker in PE.

INTRODUCTION

Preeclampsia (PE) is a significant cause of maternal and perinatal morbidity and mortality worldwide, accounting for approximately one in five maternal deaths and 15%–20% of all premature deliveries.[1] According to one estimate, women who had PE in their pregnancies have a significantly increased rate of cardiovascular disease in the future.[2,3] These women who were affected by PE had higher risk for heart failure, stroke, and death as a result of cardiovascular disease compared with women who had uncomplicated pregnancies.[3] Furthermore, the rate of long-term cardiovascular morbidity is associated with the severity and the gestational age of onset of PE. Although the exact mechanism of placental-related disorders is yet to be understood, it is believed that inadequate trophoblastic invasion plays a role in the pathogenesis of PE and other disorders. Impaired development of the placenta translates into persistently elevated resistance to blood flow in the uteroplacental circulation.[4,5]

Long noncoding RNAs (lncRNAs) are a class of noncoding RNAs that are at least 200 nt long.[6] Given the biochemical versatility of RNA, lncRNAs play a functional role in various biological processes,[7,8] including post-transcriptional regulation, organization of protein complexes, cell-cell signaling and allosteric regulation of proteins.[9,10] lncRNA hypoxia-inducible factor 1 alpha-antisense RNA 2 (HIF1A-AS2) is a 2,051-bp lncRNA that is located in the chromosome 14q23.2. Recent studies have shown that HIF1A-AS2 may have been involved in the progression of a variety of tumors, including gastric carcinomas,[11] bladder cancer,[12] colorectal cancer[13] and glioblastoma multiforme.[14] However, a few studies reported that HIF1A-AS2 may be associated with the development of PE and that its dysregulation may participate in disease progression. The biological functions of HIF1A-AS2 in the control of PE pathogenesis have not been well illustrated. Furthermore, the molecular interactions of HIF1A-AS2 also remain poorly understood. These unanswered questions compelled us to investigate the role of HIF1A-AS2 in the development of PE.

In this study, we explored the potential molecular mechanisms underlying the relationship between HIF1A-AS2 and PE progression. We found that HIF1A-AS2 was significantly downregulated in PE tissues compared with normal pregnant placenta tissues and may be an independent predictor for the development of PE. In addition, HIF1A-AS2 could regulate cell proliferation, invasion, and migration. We demonstrated that HIF1A-AS2 was associated with lysine-specific demethylase 1 (LSD1), and that this association was required for the epigenetic repression of pleckstrin homology-like domain, family A, member 1 (PHLDA1), which plays a significant role in the

Received 25 December 2018; accepted 11 April 2019;
https://doi.org/10.1016/j.omtn.2019.04.009.

[6]These authors contributed equally to this work.

Correspondence: Lizhou Sun, Department of Obstetrics and Gynecology, First Affiliated Hospital of Nanjing Medical University, Nanjing 210029, Jiangsu Province, China.
E-mail: lizhou_sun@163.com

Table 1. Clinical Characteristics of Patients with PE and Normal Pregnancies

Variable	PE (N = 52)	Control (N = 52)	p Value (PE versus Control)
Maternal age (year)	32.154 ± 5.622	33.75 ± 3.792	>0.05
Maternal weight (kg)	74.760 ± 10.812	72.135 ± 8.967	>0.05
Smoking	0	0	>0.05
Systolic blood pressure (mm Hg)	158.712 ± 24.498	115.808 ± 7.758	<0.01
Diastolic blood pressure (mm Hg)	104.250 ± 11.216	74.115 ± 8.375	<0.01
Proteinuria (g/day)	>0.3	<0.3	<0.05
Body weight of infant (g)	2,366.346 ± 865.652	3,411.538 ± 365.100	<0.05

activation-induced apoptosis.[15] In summary, we may offer new insights into the critical role of the lncRNA HIF1A-AS2 in modulating human PE.

RESULTS

HIF1A-AS2 Is Downregulated in Placental Tissue in Patients with PE

We analyzed the clinical characteristics of 104 participants (Table 1). The results indicated that systolic and diastolic blood pressure and proteinuria were higher in PE patients compared with patients with normal pregnancies. The body weight of neonates from PE pregnancies was lower because of the higher rate of early termination in PE pregnancies, which were included in the analysis.

Next, we analyzed the expression levels of HIF1A-AS2 in 52 pairs of PE samples and adjacent normal samples with normalization to GAPDH by quantitative real-time PCR assay. The expression levels of HIF1A-AS2 in PE were significantly lower ($p < 0.05$) in 76.9% (40/52) of the samples compared with the corresponding normal counterparts (Figure 1A). Furthermore, as shown in Figure 1B, 52 PE patients were divided into two groups according to the median value of their HIF1A-AS2 expression levels: a high-HIF1A-AS2 group (above the median, n = 12) and a low-HIF1A-AS2 group (below the median, n = 40). Also, we found that HIF1A-AS2 was lower in PE with about 2.2-fold downregulation as shown in Figure 1C.

Then, we analyzed HIF1A-AS2 expression in four trophoblast cell lines (HTR-8/SVneo, BeWo, JEG3, and JAR) (Figure 1D). We chose cell lines with relatively high HIF1A-AS2 expression (HTR-8/SVneo and JAR) to explore its functional activity.

To assess HIF1A-AS2 effects in trophoblasts, we knocked down or overexpressed HIF1A-AS2 in HTR-8/SVneo and JAR cells by transfecting with siRNA or with overexpression plasmid (pcDNA3.1-HIF1A-AS2), respectively. As shown in Figure 1E, HIF1A-AS2 expression was silenced in HTR/SVneo and JAR cells more efficiently by si-HIF1A-AS2-1# and si-HIF1A-AS2-2# by analyzing quantitative real-time PCR data.

So, we primarily utilized si-HIF1A-AS2-1# and si-HIF1A-AS2-2# to investigate potential mechanisms in subsequent experiments. The upregulation of HIF1A-AS2 expression by transfecting pcDNA3.1-HIF1A-AS2 plasmid was confirmed in two cell lines (Figure 1F).

HIF1A-AS2 Can Promote Proliferation of Trophoblasts and Affect Cell Cycle and Apoptosis in Trophoblasts

Knockdown of HIF1A-AS2 expression by transfecting with si-HIF1A-AS2 significantly suppressed proliferation activity in HTR-8/SVneo and JAR cells as evidenced by the Cell Counting Kit-8 (CCK-8) assay (Figures 2A and 2C). The effect described above was reversed by HIF1A-AS2 overexpression, which significantly promoted cell proliferation (Figures 2B and 2D). Further, the results of ethynyl deoxyuridine (EdU) immunostaining confirmed the above findings (Figures 2E and 2F). Collectively, these results indicate that HIF1A-AS2 positively regulates the proliferation of HTR/SVneo and JAR trophoblast cells. The results suggest that knockdown of HIF1A-AS2 can play a vital role in the development of PE.

Furthermore, we wanted to explore whether HIF1A-AS2 impacts the proliferation of HTR-8/SVneo and JAR cells through cell-cycle regulation. To investigate this, we tested cell-cycle progression using flow cytometric analysis. The knockdown of HIF1A-AS2 resulted in cell-cycle arrest at the G0/G1 phase (Figures 3A and 3C), whereas HIF1A-AS2 overexpression reversed the effect (Figures 3B and 3D). Consistent with these results, the apoptosis rate in HTR/SVneo and JAR trophoblasts increased after HIF1A-AS2 knockdown by siRNAs (Figure 3E). The phenomena revealed that HIF1A-AS2 was involved in the regulation of cell-cycle progression and apoptosis in trophoblasts.

HIF1A-AS2 Influences the Function of Migration and Invasion Ability of Trophoblasts *In Vitro*

Next, we evaluated the effects of HIF1A-AS2 on the migration and invasion abilities of HTR-8/SVneo and JAR cells using the Transwell assays. Proper trophoblast migration and invasion are important for the establishment of the blood flow between the mother and embryo, and the development of this placental vasculature is impaired in PE patients. Accordingly, knockdown of HIF1A-AS2 inhibited trophoblast migration and invasion (Figures 3F and 3H), whereas HIF1A-AS2 overexpression exhibited the opposite effect (Figures 3G and 3I). These results suggest that HIF1A-AS2 may influence trophoblast migration and invasion.

HIF1A-AS2 Influences Gene Expression in Trophoblasts

We performed RNA transcriptome sequencing to explore HIF1A-AS2-associated changes in gene expression in negative control siRNA (si-NC) and si-HIF1A-AS2-transfected HTR/SVneo cells. A total of 277 and 342 transcripts were increased or decreased, respectively (Figure 4A; Table S2). Evaluation of the biological pathways activated by HIF1A-AS2 using Gene Ontology (GO) and Kyoto Encyclopedia

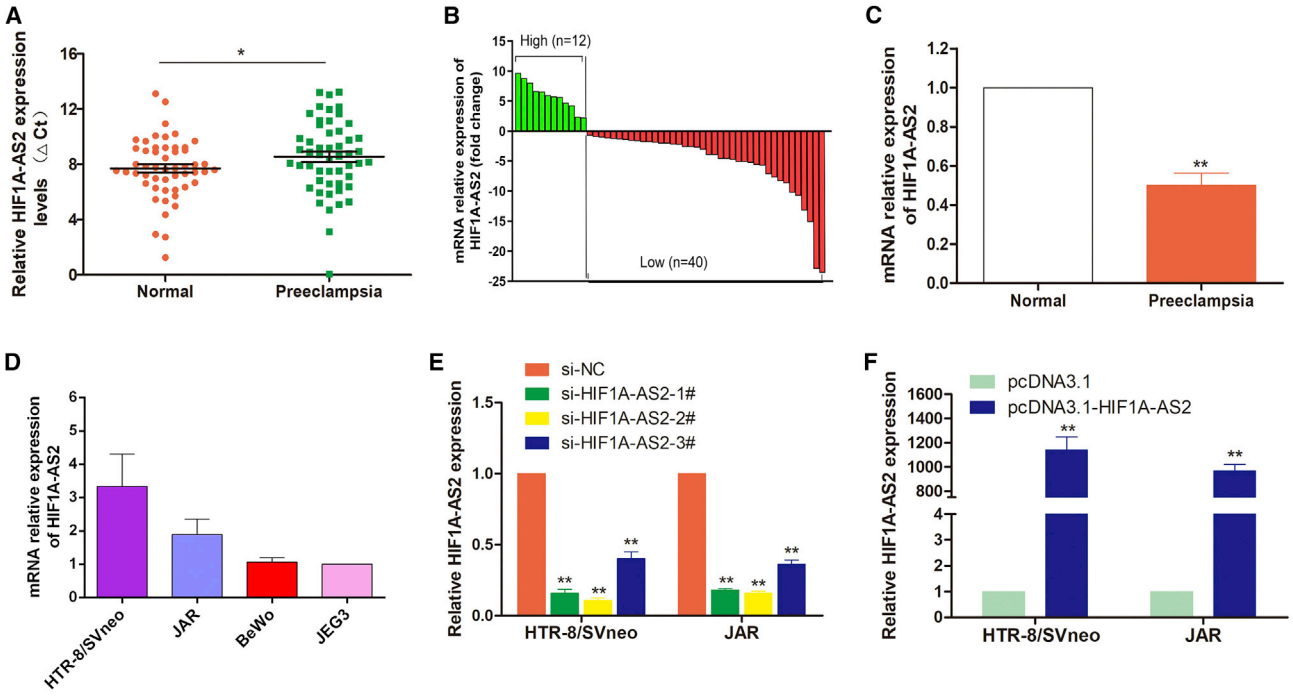

Figure 1. HIF1A-AS2 Expression Is Decreased in PE

(A–C) The expression of HIF1A-AS2 was analyzed by quantitative real-time PCR and normalized to that of GAPDH. (A) Relative expression levels of HIF1A-AS2 in PE tissues (n = 52) compared with corresponding normal tissues (n = 52). The ΔCt value was determined by subtracting the GAPDH Ct value from the HIF1A-AS2 Ct value (relative to a single reference value). Higher ΔCt values indicate smaller expression. (B) HIF1A-AS2 levels were lower in PE placentas (n = 52) compared with normal placentas (n = 52). (C) Results are presented as the 2.2-fold change in PE placental samples relative to the control, and HIF1A-AS2 expression was classified into two groups. (D) HIF1A-AS2 expression in trophoblast cell lines analyzed by quantitative real-time PCR. The levels of HIF1A-AS2 in HTR-8/SVneo, BeWo, and JAR cell lines were normalized to that in JEG3. (E and F) Relative HIF1A-AS2 expression in HTR-8/SVneo and JAR cells transfected with HIF1A-AS2 siRNAs (E) and pcDNA3.1-HIF1A-AS2 (F). The data are presented as the mean ± SD of three independent experiments; *p < 0.05, **p < 0.01.

of Genes and Genomes (KEGG) databases indicated that genes related to cell growth were changed in HIF1A-AS2-knockdown cells (Figure 4B). Expression changes in HTR-8/SVneo and JAR cells were further confirmed by quantitative real-time PCR. Transcripts related to cell growth, apoptosis and migration of the expression of PHLDA1 were significantly upregulated after HIF1A-AS2 knockdown in HTR-8/SVneo and JAR cells (Figures 4C and 4D). Also, western blot analysis discovered the similar effects of HIF1A-AS2 on PHLDA1 protein expression in HTR-8/SVneo and JAR cells (Figure 4E). PHLDA1 encodes an evolutionarily conserved proline-histidine-rich nuclear protein.

Although PHLDA1 has been shown to be both pro-apoptotic and antiapoptotic depending on the cell line and the experimental conditions, PHLDA1 is essential for rescuing cells from serum starvation-induced apoptosis in NIH 3T3 cells expressing insulin-like growth factor 1 (IGF1) receptors.[16] Conversely, in T cells, neuronal, endothelial, melanoma, cervical carcinoma, and other cell lines, PHLDA1 plays a role in reducing proliferation and inducing cell death.[17] Also, reduced PHLDA1 expression has been described in some cancers, and current data indicate that PHLDA1 may act as an apoptotic gene.

HIF1A-AS2 Silences PHLDA1 Epigenetically by Binding to LSD1

To further examine the effects of HIF1A-AS2 on gene expression, we investigated the subcellular localization of HIF1A-AS2 in HTR/SVneo and JAR cells using GAPDH and small nuclear RNA U1 (RNU1) as cytoplasmic and nuclear markers, respectively, subcellular fractionation, and RNA isolation assays (Figures 5A and 5B). The results indicate that HIF1A-AS2 was mainly localized in the cell nucleus, supporting its role in transcriptional regulation.

Recently, it was reported that by regulating target gene expression, LSD1 can influence tumorigenesis, embryonic differentiation and the formation of euchromatin.[18,19] Therefore, we hypothesized that HIF1A-AS2 may control PHLDA1 expression by recruiting LSD1 in trophoblasts. Indeed, the RNA immunoprecipitation (RIP) assay showed that HIF1A-AS2 was precipitated with anti-LSD1 antibodies in HTR-8/SVneo and JAR cells (Figures 5C and 5D).

We then investigated the potential functional relationship between HIF1A-AS2 and LSD1. The knockdown of LSD1 by a specific siRNA resulted in PHLDA1 upregulation both at the protein and mRNA

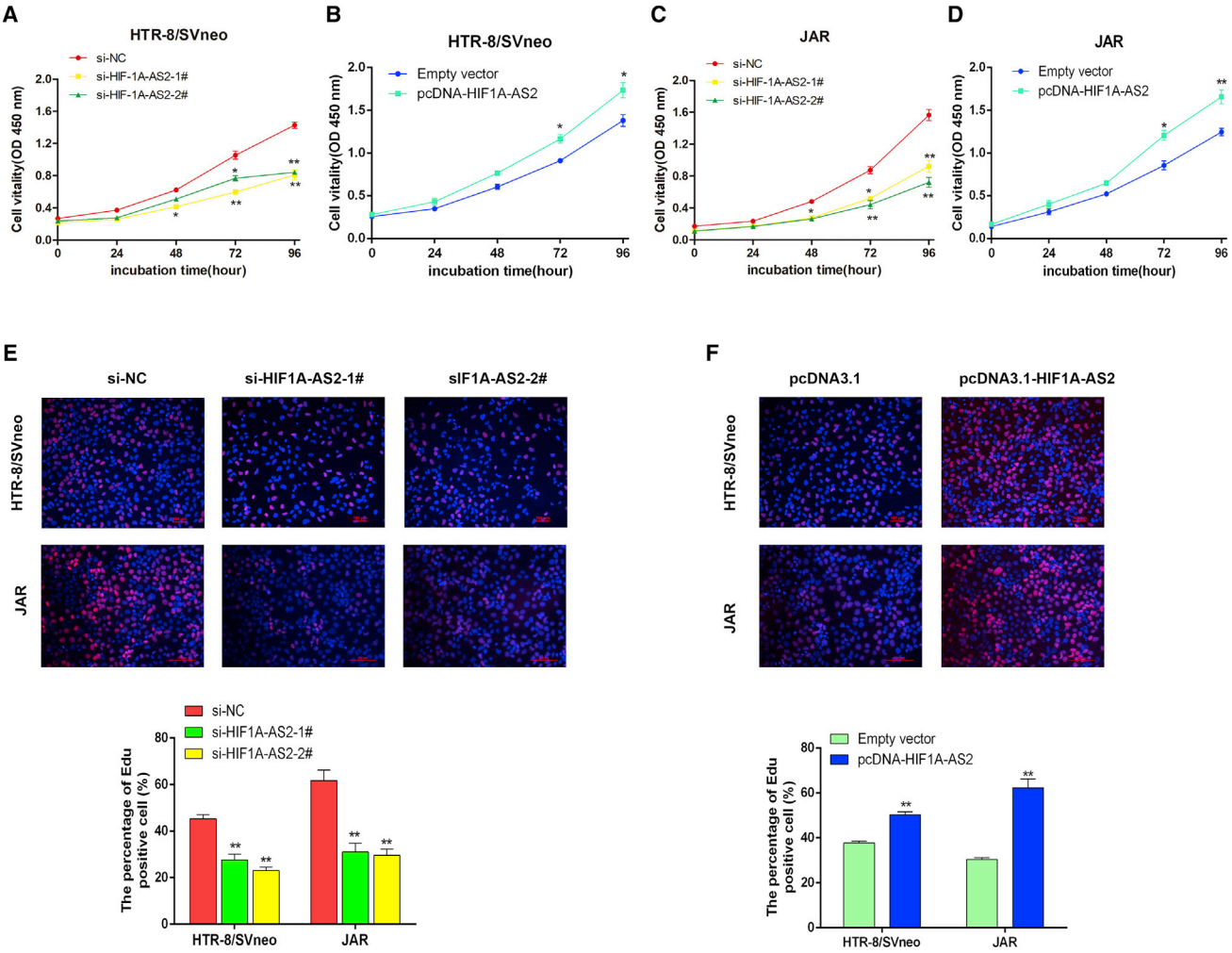

Figure 2. HIF1A-AS2 Promotes Trophoblast Proliferation *In Vitro*

(A–D) The viability of si-HIF1A-AS2-transfected HTR-8/SVneo (A) and JAR (C) cells or pCDNA3.1-HIF1A-AS2-transfected HTR-8/SVneo (B) and JAR (D) cells was analyzed by the CCK-8 assay. (E and F) Proliferating HTR-8/SVneo and JAR cells with si-HIF1A-AS2-transfected (E) and pcDNA3.1-HIF1A-AS2-transfected (F) cells are marked with EdU (red) and cell nuclei are stained with DAPI (blue). The data are presented as the mean ± SD of three independent experiments; *$p < 0.05$, **$p < 0.01$.

levels (Figures 5E–5G), suggesting that HIF1A-AS2 may regulate PHLDA1 expression in trophoblasts through epigenetic mechanisms. The chromatin immunoprecipitation (ChIP) assay with antibodies against LSD1 and H3K4me2 revealed the enrichment of LSD1 and H3K4me2 in the promoter region of the PHLDA1 gene, which was significantly decreased for LSD1 but increased for H3K4me2 after transfection with si-HIF1A-AS2 (Figures 5H and 5I).

PHLDA1 Upregulated in PE Placental Tissues Influences Trophoblast Viability *In Vitro*

Evaluation of PHLDA1 mRNA expression in 40-pair low-HIF1A-AS2 group placental tissues of PE patients indicated that PHLDA1 transcription was increased in PE compared with normal pregnancy (Figure 6A). In HTR-8/SVneo and JAR trophoblasts, PHLDA1 knockdown promoted cell proliferation by CCK-8 (Figures 6B and 6C) and Edu assays (Figure 6D). Finally, we examined the biological effects of PHLDA1 association with HIF1A-AS2 by co-transfecting HTR-8/SVneo and JAR cells with si-HIF1A-AS2 and PHLDA1 siRNAs, and analyzing cell proliferation using CCK-8 assays (Figures 6E and 6F). The results indicated that si-PHLDA1 could moderately rescue si-HIF1A-AS2-mediated inhibition of proliferation in HTR-8/SVneo and JAR cells.

DISCUSSION

LncRNAs are noncoding RNAs expressed at lower levels compared with protein-coding transcripts and can be either nuclear, nucleolar, or cytoplasmic. LncRNAs in the nucleus have functions in histone modification and block the binding of transcription factors to their promoters or direct transcriptional regulation.[10,20] More than 200 diseases are related to dysregulated or dysfunctional lncRNAs. They can act as

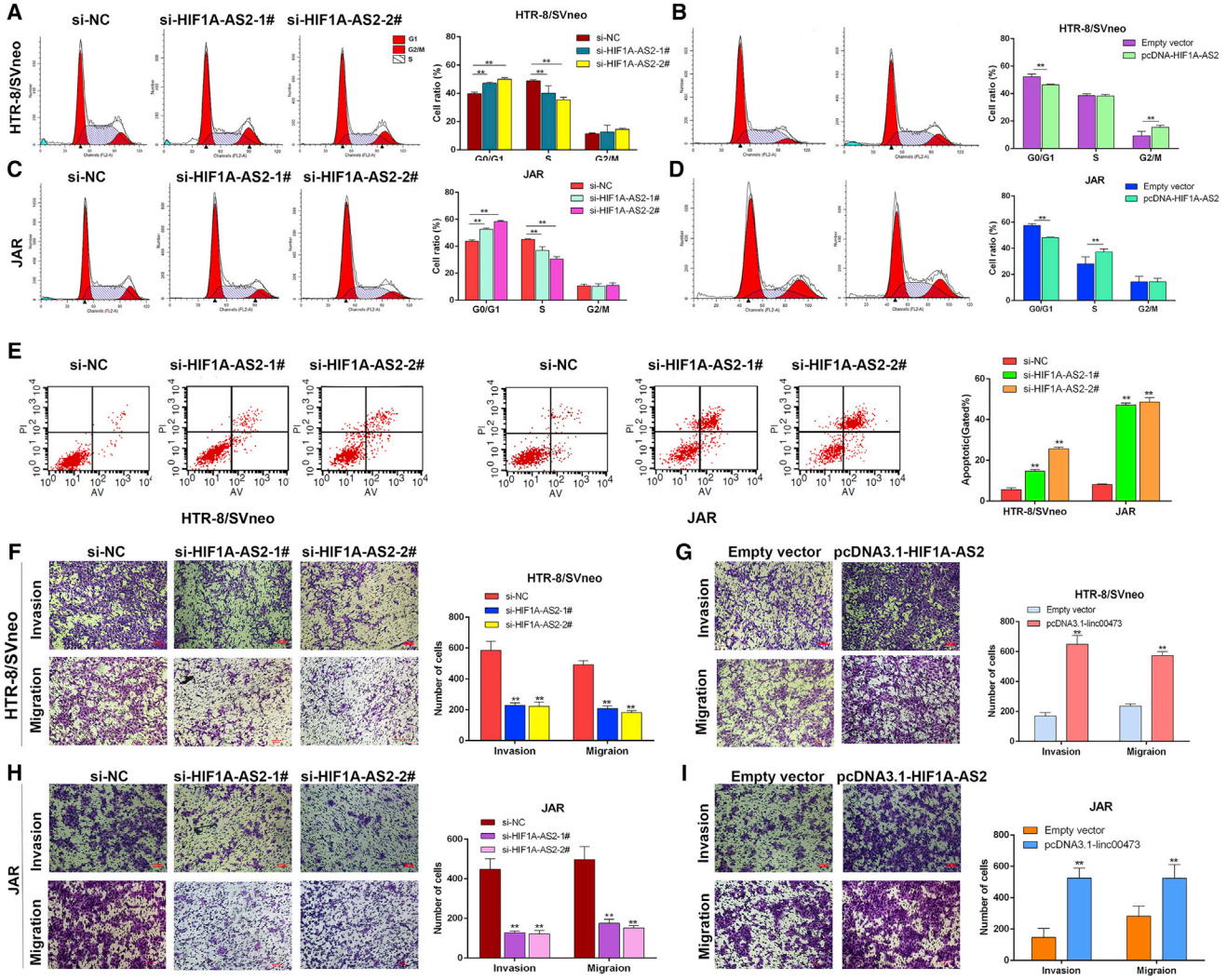

Figure 3. Effects of HIF1A-AS2 on Trophoblast Cell Cycle, Apoptosis, Migration, and Invasion *In Vitro*

HTR-8/SVneo and JAR trophoblasts were transfected with HIF1A-AS2-specific siRNAs (si-HIF1A-AS2-1# and si-HIF1A-AS2-2#) or were transfected with pcDNA3.1-HIF1A-AS2. (A–D) Cell cycle was analyzed by flow cytometry in HTR-8/SVneo (A and B) and JAR (C and D) cells. Representative FACS images and related statistics are shown. (E) Cell apoptosis rates were analyzed by flow cytometry. The data are presented as the mean ± SD of three independent experiments; *$p < 0.05$, **$p < 0.01$. (F–I) The migration and invasion capacity of cultured trophoblasts transfected with si-HIF1A-AS2 in HTR-8/SVneo cells (F) and JAR (H) or pcDNA3.1-HIF1A-AS2 in HTR-8/SVneo (G) and JAR (I) cells and analyzed by the Transwell assays was significantly lower or higher, respectively, than that of control cells. The data are presented as the mean ± SD of three independent experiments; **$p < 0.01$. LR, early apoptotic cells; UR, terminal apoptotic cells.

structural scaffolds of nuclear domains and influence chromatin organization, as well as transcriptional and post-transcriptional regulation of gene expression.[21] Thus, exploration and identification of PE-associated lncRNAs and their functions may provide a new angle in the understanding of PE pathogenesis and define novel therapeutic targets, as well as provide diagnostic and prognostic markers for PE.

The extra-villous trophoblasts (EVTs) play a role in migrating through the endometrium, invade the uterine decidua, meeting only little resistance, and remodel the spiral arteries to establish appropriate nutrient and oxygen supplies for the fetus during the success of pregnancy.[22] EVTs are functional cells and may be crucial in the placenta, and the abnormal proliferation, apoptosis, and invasion of EVTs are pivotal contributors to the failure of placentation. EVTs also display a phenotype very similar to that of cancer cells, regarding their capacity for proliferation, apoptosis, migration, and invasion.[23] PE is a multi-factorial disease that is caused by the interaction of both genetic and environmental factors.[24,25] However, some of the specific mechanisms underlying the pathogenesis of the disease are unclear. The abnormal invasion of trophoblast cells in the placenta disc and the disturbance of recasting the spiral artery are the important reasons behind the insufficiency of the blood circulation in the placenta

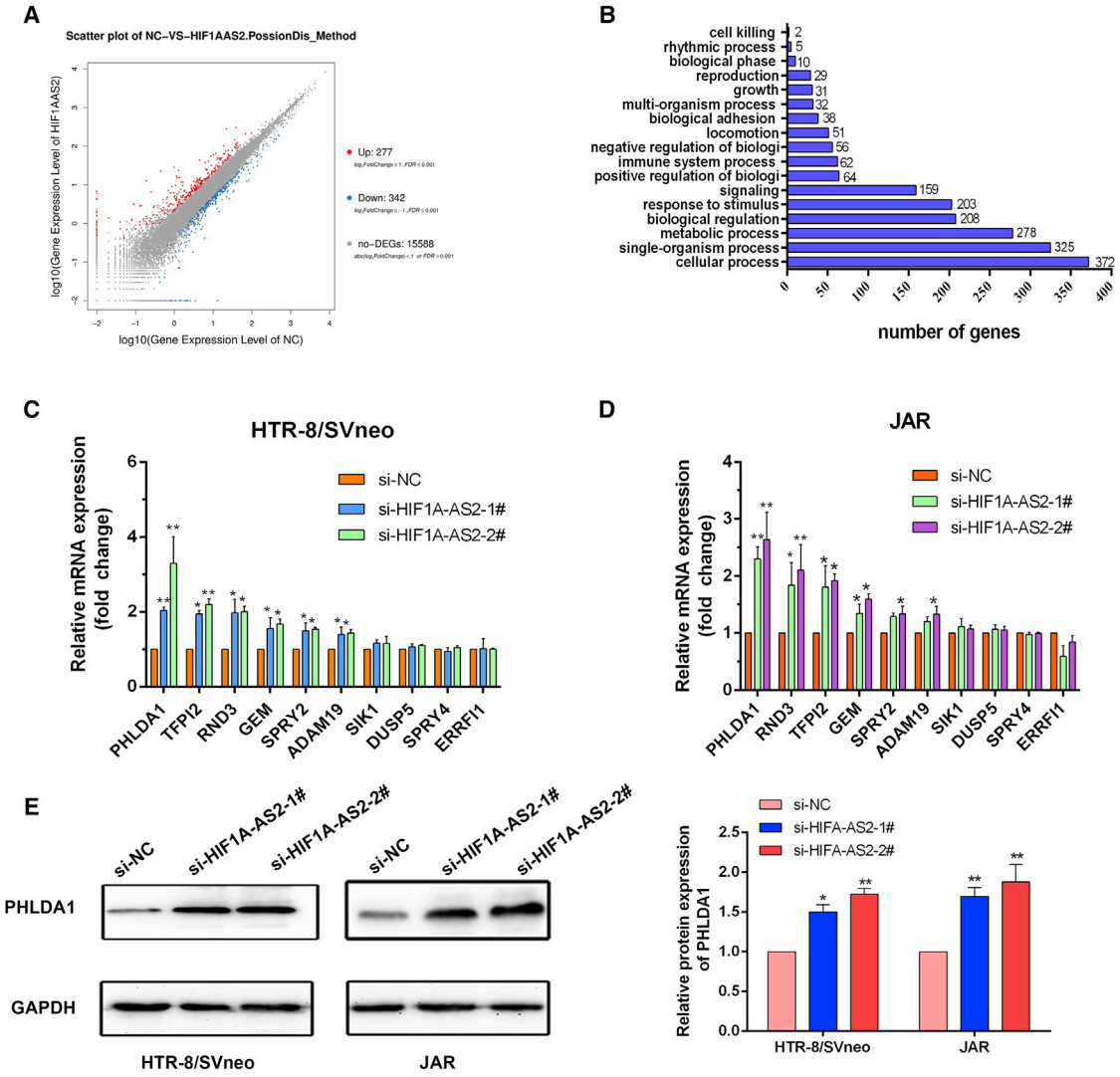

Figure 4. HIF1A-AS2 Knockdown Affected the Expression of Genes Involved in Cell Proliferation and Migration

(A and B) Gene expression profiling was performed by RNA-seq in HTR-8/SVneo cells transfected with si-HIF1A-AS2. Differentially expressed genes are shown (A). GO analysis of genes differentially expressed in si-NC- and si-HIF1A-AS2-transfected cells. Cell growth was among significant biological processes affected by HIF1A-AS2 depletion in trophoblasts as evidenced by the number of genes with altered expression (B). (C and D) Relative mRNA expression of genes involved in cell proliferation and migration in HIF1A-AS2-deficient HTR-8/SVneo cells (C) and JAR cells (D) was analyzed by quantitative real-time PCR. (E) PHLDA1 protein expression in HIF1A-AS2-deficient HTR-8/SVneo cells and JAR cells was assessed by western blotting. The data are presented as the mean ± SD of three independent experiments; *$p < 0.05$, **$p < 0.01$.

typically seen in PE.[26] These aspects can partly explain the pathogenesis of PE and help us to further explore it.

In our study, we explored the potential molecular mechanism of HIF1A-AS2 mainly using several different trophoblastic cell lines as a model system. HIF1A-AS2 has been mainly investigated for its role in cancer. In this study, we found that expression of HIF1A-AS2 was downregulated in the placental tissues of women with PE compared with women with normal pregnancies. *In vitro*, silencing of HIF1A-AS2 expression can effectively suppress the proliferation, cell-cycle progression, invasion, and migration of trophoblast cells, whereas HIF1A-AS2 overexpression caused the opposite results. These findings implicate HIF1A-AS2 as an important regulatory molecule involved in the control of the biological activity of the main players' PE pathogenesis and suggest that HIF1A-AS2 may be a promising biomarker for the diagnosis of PE.

PHLDA1 was first identified as a potential transcription factor required for Fas expression and activation-induced apoptosis in mouse T cell hybridomas.[27] The exact molecular and biological

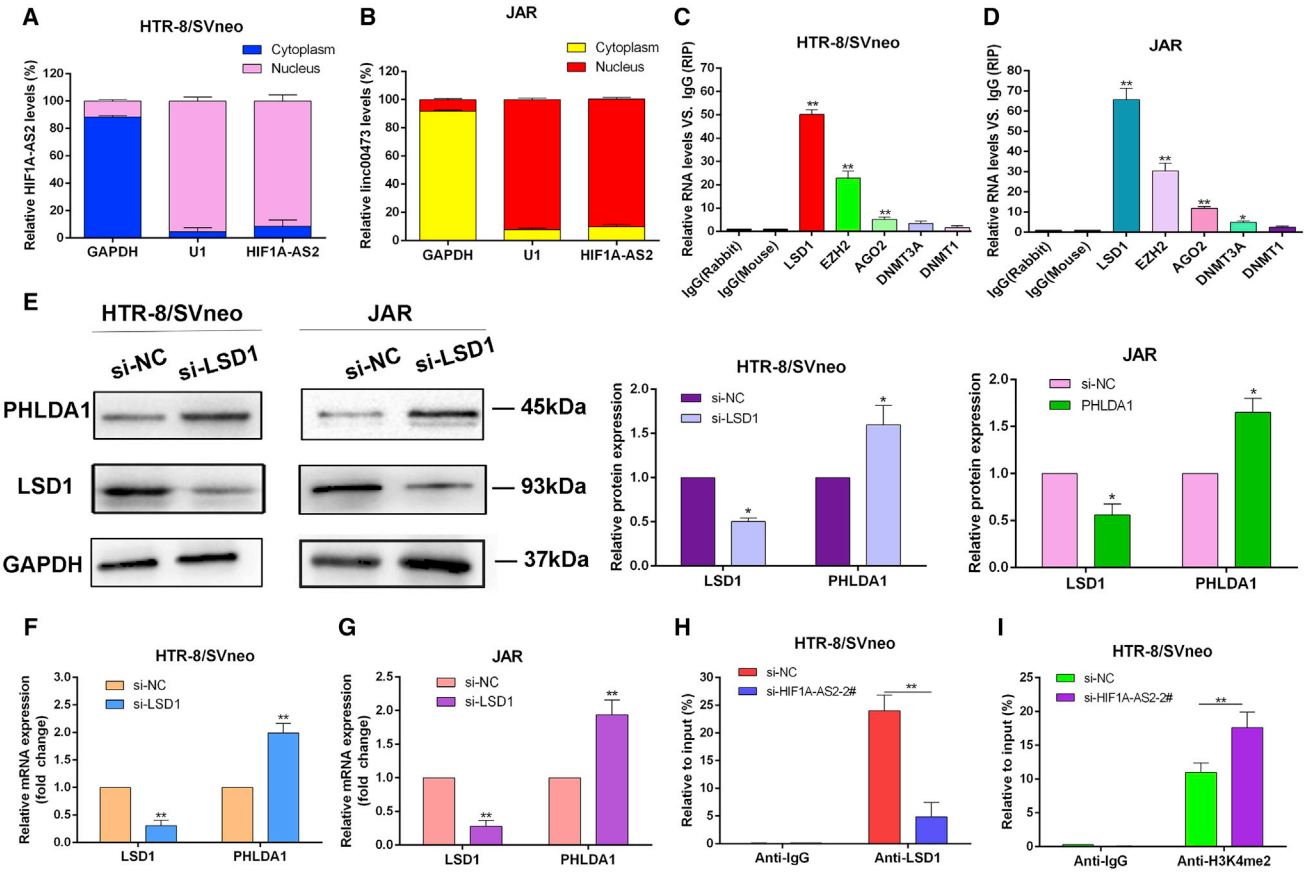

Figure 5. HIF1A-AS2 Binding to LSD1 Inhibits PHLDA1 Expression

(A and B) Cell fractionation assay revealed that HIF1A-AS2 was predominantly localized in the nucleus of HTR-8/SVneo (A) and JAR (B) cells. GAPDH and small nuclear RNA U1 were used as cytoplasmic and nuclear markers, respectively. (C and D) RIP assays showed that HIF1A-AS2 was mainly bound to LSD1 in HTR-8/SVneo cells (C) and JAR (D) cells, respectively. (E–G) LSD1 silencing changed the expression of LSD1 and PHLDA1 at the protein (E) and mRNA (F and G) levels in HTR-8/SVneo and JAR cells. (H and I) Enrichment of LSD1 (H) and H3K4me2 (I) in the promoter region of PHLDA1 detected by the ChIP assay. The data are presented as the mean ± SD of three independent experiments; *$p < 0.05$, **$p < 0.01$.

functions of PHLDA1 remain to be elucidated. However, its expression is induced by a variety of external stimuli, and there is evidence that it may function as a transcriptional activator that acts as a mediator of apoptosis,[28] proliferation, differentiation,[29] and cell migration[30] dependent on the cellular type and context. Recently, PHLDA1 has received attention because of its association with cancer.[31–33] Consistent with these findings, PHLDA1 knockdown promoted proliferation of cultured trophoblasts and counterbalanced the inhibitory effects of HIF1A-AS2 deficiency. Our results also indicate that PHLDA1 expression was silenced by LSD1 through epigenetic mechanisms. Based on these findings, we propose that HIF1A-AS2 can inhibit PHLDA1 expression by binding to LSD1 in trophoblasts, thus promoting their invasion and migration, the critical processes for proper uterine spiral artery remodeling in pregnancy, which are deregulated in PE.

In conclusion, this study discovered that the role of HIF1A-AS2 may be as a scaffold and an important indicator of the LSD1-mediated epigenetic regulatory pathway participating in the inhibition of PHLDA1 expression during the development of PE. The present findings show that HIF1A-AS2 can be a novel molecular target for earlier diagnosis and treatment of PE (Figure 6G). Further studies are needed to elucidate other potential mechanisms through which HIF1A-AS2 participates in the biological functions of trophoblasts in the context of PE.

MATERIALS AND METHODS

Patients and Collection of Tissue Samples

We obtained 52 paired placental samples from women with normal pregnancies and PE who underwent cesarean deliveries in Jiangsu Province Hospital from August 2016 to December 2018. The placenta tissue samples (about 1 cm × 1 cm × 1 cm in size) were taken from the central area of the placenta maternal surface to avoid necrosis and calcification, and were immediately frozen in liquid nitrogen and subsequently used for RNA and protein extraction. Clinicopathological characteristics of the participants are summarized in Table 1. This

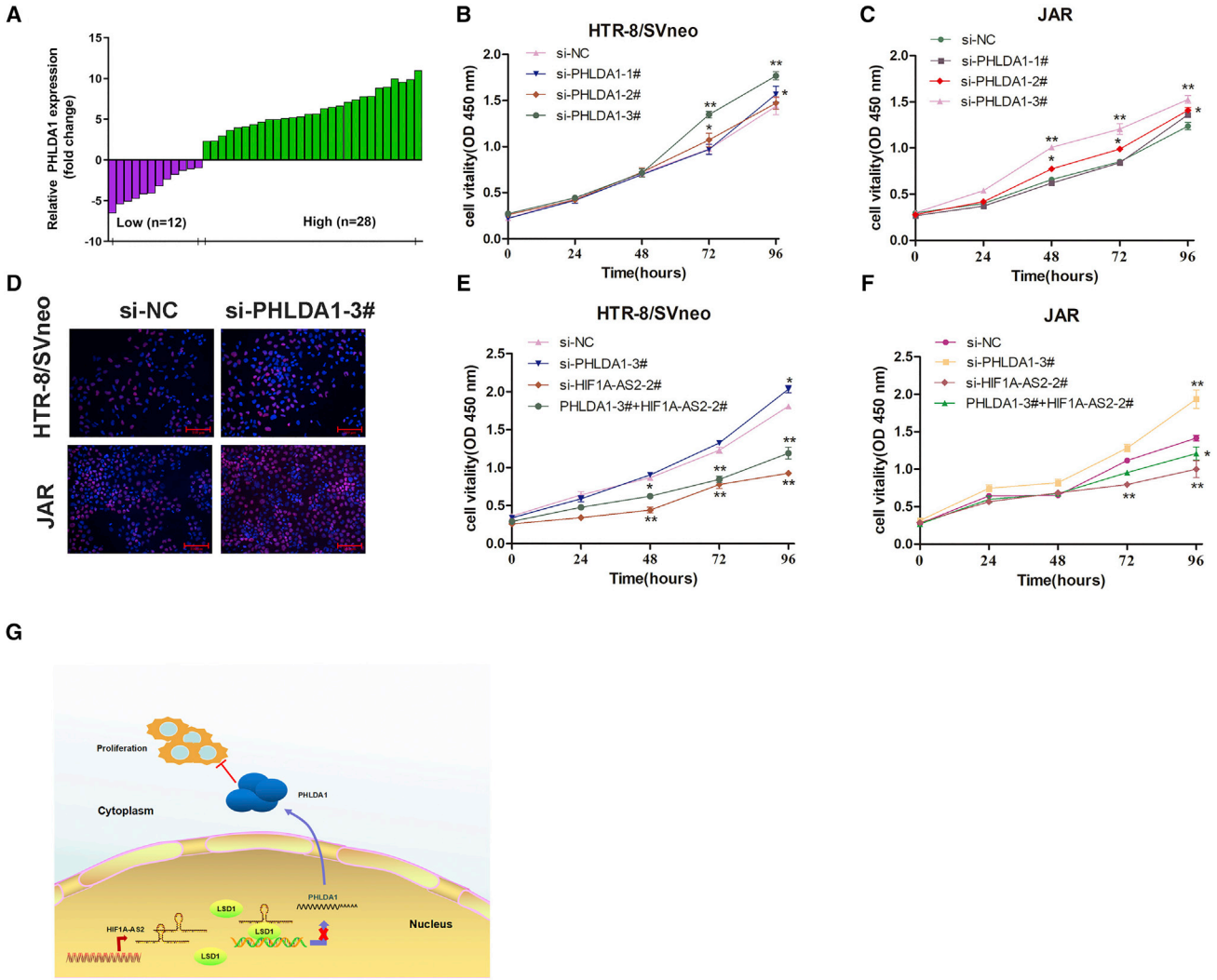

Figure 6. PHLDA1 Inhibits Trophoblast Proliferation and Counterbalances the Activity of HIF1A-AS2

(A) Relative expression of PHLDA1 (fold-change) in placental tissues of PE patients compared with those of healthy pregnant women (n = 32). (B and C) CCK-8 assay analysis of cell viability for si-PHLDA1 transfected in HTR-B/SVneo (B) and JAR (C) trophoblasts. (D) Proliferation of HTR-8/SVneo and JAR cells analyzed by the EdU assays. (E and F) Cell proliferation ability was analyzed using CCK-8 assays by co-transfecting HTR-8/SVneo (E) and JAR (F) cells with si-HIF1A-AS2-2# and si-PHLDA1-3#. The data are presented as the mean ± SD of three independent experiments; *$p < 0.05$, **$p < 0.01$. (G) A potential schematic pathway illustrating the role of HIF1A-AS2 in the proliferation and migration of trophoblasts in PE.

research was authorized by the Ethnics Board of the First Affiliated Hospital of Nanjing Medical University, China, and all patients provided written informed consent.

Cell Culture

Four human trophoblast cell lines (HTR/SVneo, JAR, JEG3, and BeVo) and human umbilical vein endothelial cells (HUVECs) were purchased from the Type Culture Collection of the Chinese Academy of Sciences (Shanghai, China). HTR/SVneo and JAR cells were cultured in RPMI 1640, JEG3 cells in MEM, BeVo cells in F12K supplemented with 10% fetal bovine serum (FBS; GIBCO BRL, Invitrogen, Carlsbad, CA, USA), 100 U/mL penicillin, and 100 mg/mL streptomycin (Invitrogen). All cells were maintained in a humidified atmosphere with 5% CO_2 at 37°C.

Cell Transfection

Plasmid vectors (pcDNA, pcDNA3.1-HIF1A-AS2, and pcDNA3.1-PHLDA1) were purified using the DNA Midiprep kit (QIAGEN, Hilden, Germany). Three different HIF1A-AS2-specific siRNAs, LSD1 and PHLDA1 siRNAs and scrambled si-NC, were purchased from Invitrogen; the sequences are shown in Table S1. HTR/SVneo, JAR, and JEG3 cells were cultured in six-well plates until 80% confluence and then transfected with siRNAs using Lipofectamine 2000 (Invitrogen, USA) or with plasmid vectors (4 μg) using

X-tremeGENE HP DNA Transfection Reagent (Roche, Pennsburg, Germany) following the manufacturers' instructions. Cells were harvested 48 h post-transfection and analyzed by real-time qPCR and western blotting.

RNA Preparation and Quantitative Real-Time PCR

Total RNA was isolated from tissues or cultured cells with TRIzol reagent (Invitrogen), and its quality and quantity were assessed using NanoDrop2000c (Thermo Fisher Scientific, Waltham, MA, USA). RNA was reverse-transcribed to cDNA using Primer Script RT Master Mix (Takara, Dalian, China), and quantitative real-time PCR was performed with SYBR Premix Ex Taq (Takara, Dalian, China) and specific primers (Table S1) in an ABI 7500 system following the manufacturer's protocol. The expression level of HIF1A-AS2 was calculated by the $2^{-\Delta\Delta CT}$ method, normalized to that of glyceraldehyde-3-phosphate dehydrogenase (GAPDH), and converted to fold changes.

Subcellular Fractionation and RNA Isolation

HTR-8/SVneo and JAR cells were washed with PBS twice. Then, cytoplasmic and nuclear RNA were separated and purified using the PARIS Kit (Life Technologies, Carlsbad, CA, USA) according to the manufacturer's instructions.

Cell Proliferation Assays

Cell proliferation of HTR/SVneo or JAR cells were seeded in 96-well plates (3,000–4,000 cells/well) and transfected with si-HIF1A-AS2 or pcDNA-HIF1A-AS2; five replicates for each point were used. Cell viability was assessed every 24 h using the CCK-8 (Roche) based on the absorbance at 450 nm measured in an ELx-800 University Microplate Reader (Biotech, Winooski, VT, USA). At least three independent experiments were performed.

EdU Assay

The EdU assay was performed for accurate estimation of cell proliferation as a complementary method using the 5-ethynyl-2-deoxyuridine labeling/detection kit (Ribobio, Guangzhou, China). HTR/SVneo and JAR cells were seeded in 24-well plates at ~$2–3 \times 10^4$ cells per well and transfected with si-HIF1A-AS2-1#, si-HIF1A-AS2-2#, si-NC, pcDNA-HIF1A-AS2, or pcDNA for ~24–48 h. Then, 200 μL/well of EdU labeling medium was added, and cells were cultured for another 2 h, fixed in 4% paraformaldehyde (pH 7.4) for 30 min, permeabilized with 0.5% Triton X-100 for 20 min at room temperature, washed in PBS (pH 7.4), and stained with anti-EdU solution for 30 min. After counterstaining with 250 μL DAPI (Invitrogen, Molecular Probes, Eugene, OR, USA) for 25 min, images of EdU-positive cells were captured under a fluorescence microscope (Nikon Corporation, Tokyo, Japan). The experiment was independently repeated three times.

Flow Cytometry Analysis of Cell Cycle and Apoptosis

Cells transfected with si-HIF1A-AS2 or pcDNA-HIF1A-AS2 were harvested about ~32–48 h post-transfection by trypsinization, washed twice with PBS, stained with propidium iodide (PI) using the Cycle TEST PLUS DNA Reagent Kit (BD Biosciences, San Jose, CA, USA), and analyzed in a FACScan flow cytometer (BD Biosciences) equipped with Cell Quest software (BD Biosciences) to estimate the percentage of cells in G0/G1, S, and G2/M phases. All samples were assayed in triplicate. Apoptosis was assessed by flow cytometry after double staining of the transfected cells with fluorescein isothiocyanate (FITC)-Annexin V and PI using the FITC-Annexin V Apoptosis Detection Kit (BD Biosciences), and the percentages of viable, dead, and early and late apoptotic cells were calculated and compared with those in controls.

Cell Migration and Invasion Assays

Cell migration and invasion assays were performed using 24-well Transwell chambers with 8-μm pore size polycarbonate membranes (Corning, Corning, NY, USA). Cells were plated on the top side of the membrane pre-coated or not with Matrigel (BD, Franklin Lakes, NJ, USA) for invasion or migration assays, respectively. After incubation for ~36–48 h, cells inside the upper chamber were removed with cottons swabs, whereas those on the lower membrane surface were fixed by methanol and stained with 0.5% crystal violet solution. Five randomly selected fields were analyzed for each well.

Western Blotting Assay

HTR/SVneo and JAR cells cultured in six-well plates were transfected with si-HIF1A-AS2 or pcDNA-HIF1A-AS2. Following transfection, total cellular proteins were extracted with RIPA protein extraction reagent (Beyotime, Beijing, China) supplemented with protease inhibitor cocktail (Roche, Pleasanton, CA, USA) and phenylmethylsulfonyl fluoride (Roche). Proteins were separated by SDS-PAGE in 10% gels and transferred to 0.22-μm polyvinylidene difluoride membranes (Sigma), which were incubated with antibodies against LSD1 (1:1,000; CST, Danvers, MA, USA) or PHLDA1 (1:1,000; Proteintech); anti-GAPDH antibody (1:3,000; Santa Cruz, CA, USA) was used as control. The intensity of protein bands was quantified by densitometry using the Quantity One software (Bio-Rad). At least three independent experiments were performed.

RNA-Sequencing Analysis

The RNA-sequencing (RNA-seq) experiments were conducted in the Huada Genomics Institute (Wuhan, China), and the mRNA-seq library was obtained according to standard protocols (Illumina, San Diego, CA, USA). In brief, total RNA from si-NC- or si-HIF1A-AS2-1#-transfected HTR-8/SVneo cells was isolated as described above, and mRNA was purified using Dynabeads Oligo (dT) (Invitrogen Dynal) and reverse-transcribed into cDNA, which was then fragmented by nebulization to establish the mRNA-seq library.

RIP Assay

RIP assays were performed using the EZ-Magna RIP kit (Millipore, Billerica, MA, USA) according to the manufacturer's instructions. HTR-8/SVneo and JAR cells were grown in 15-cm plates, collected by centrifugation, and lysed in RIP lysis buffer so that 100 μL contained the lysate

of ~1–2.0 × 10^7 cells. Cell lysates were used for immunoprecipitation with anti-LSD1, -EZH2, -AGO2, -DNMT1, and -DNMT3A antibodies and normal immunoglobulin G (IgG; Millipore, Billerica, MA, USA), and the immunoprecipitated RNA was amplified by quantitative real-time PCR using the Primer Script RT Master Mix kit and primers specific for HIF1A-AS2 and IgG (Table S1).

ChIP Assay

ChIP assays were performed using the EZ-Magna ChIP A kit (Millipore) according to the manufacturer's protocol. HTR-8/SVneo and JAR cells were cross-linked by 1% formaldehyde for 10 min at 25°C, lysed, and sonicated to obtain 200- to 500-bp DNA fragments. Primary LSD1 and H3K4me2-specific antibodies (Millipore) or control IgG were added to pre-cleared supernatants, and the mixtures were incubated with rotation for 3 h or overnight at 4°C. Then, Dynabeads protein A/G were added to the mixtures, and the samples were incubated with vortexing for 2 h at 4°C. The beads were then washed sequentially with low-salt and high-salt RIPA, LiCi, and TE, and DNA was isolated by phenol/chloroform extraction. ChIP-qPCR was performed using SYBR Premix Ex Taq and specific primers (Table S1), and the data were normalized to the input. At least three independent experiments were conducted.

Statistical Analysis

The statistical analyses were performed with the SPSS 17.0 statistical software (IBM, Chicago, IL, USA). Each experiment was independently repeated at least three times, and the data were expressed as the mean ± SD. Student's t test or Mann-Whitney test were used for comparisons between two groups, and ANOVA or Kruskal-Wallis tests were applied for multiple comparisons. p values less than 0.05 indicated statistical significance.

SUPPLEMENTAL INFORMATION

Supplemental Information can be found online at https://doi.org/10.1016/j.omtn.2019.04.009.

AUTHOR CONTRIBUTIONS

L.S. and D.W. conceived and designed the study. D.W., N.Y. and Y.X. wrote the article. The experiments were performed by D.W., Y.X. and N.Y. The tissue samples were collected by S.W. and Y.Z. The data were coordinated and analyzed by M.S., B.H. and Z.H. All of the authors contributed to, read, and approved the final manuscript.

CONFLICTS OF INTEREST

The authors declare no competing interests.

ACKNOWLEDGMENTS

The present work was supported by the National Natural Science Foundation of China (grants 81771603 and 81801472), Postgraduate Research & Practice Innovation Program of Jiangsu Province (grant KYCX18_1481), Natural Science Foundation of Jiangsu Province (project numbers: BK20171502, BK20161061, and BK20181080), and National Key Research Plan of China (grant 2018YFC1002205).

REFERENCES

1. Pedroso, M.A., Palmer, K.R., Hodges, R.J., Costa, F.D.S., and Rolnik, D.L. (2018). Uterine Artery Doppler in Screening for Preeclampsia and Fetal Growth Restriction. Rev. Bras. Ginecol. Obstet. *40*, 287–293.

2. Groenhof, T.K.J., van Rijn, B.B., Franx, A., Roeters van Lennep, J.E., Bots, M.L., and Lely, A.T. (2017). Preventing cardiovascular disease after hypertensive disorders of pregnancy: searching for the how and when. Eur. J. Prev. Cardiol. *24*, 1735–1745.

3. Wu, P., Haththotuwa, R., Kwok, C.S., Babu, A., Kotronias, R.A., Rushton, C., Zaman, A., Fryer, A.A., Kadam, U., Chew-Graham, C.A., and Mamas, M.A. (2017). Preeclampsia and Future Cardiovascular Health: A Systematic Review and Meta-Analysis. Circ. Cardiovasc. Qual. Outcomes *10*, e003497.

4. Wallace, A.E., Fraser, R., Gurung, S., Goulwara, S.S., Whitley, G.S., Johnstone, A.P., and Cartwright, J.E. (2014). Increased angiogenic factor secretion by decidual natural killer cells from pregnancies with high uterine artery resistance alters trophoblast function. Hum. Reprod. *29*, 652–660.

5. Wallace, A.E., Whitley, G.S., Thilaganathan, B., and Cartwright, J.E. (2015). Decidual natural killer cell receptor expression is altered in pregnancies with impaired vascular remodeling and a higher risk of pre-eclampsia. J. Leukoc. Biol. *97*, 79–86.

6. Lin, P., Wen, D.Y., Li, Q., He, Y., Yang, H., and Chen, G. (2018). Genome-Wide Analysis of Prognostic lncRNAs, miRNAs, and mRNAs Forming a Competing Endogenous RNA Network in Hepatocellular Carcinoma. Cell. Physiol. Biochem. *48*, 1953–1967.

7. Delás, M.J., and Hannon, G.J. (2017). lncRNAs in development and disease: from functions to mechanisms. Open Biol. *7*, 170121.

8. Ernst, E.H., Nielsen, J., Ipsen, M.B., Villesen, P., and Lykke-Hartmann, K. (2018). Transcriptome Analysis of Long Non-coding RNAs and Genes Encoding Paraspeckle Proteins During Human Ovarian Follicle Development. Front. Cell Dev. Biol. *6*, 78.

9. Geisler, S., and Coller, J. (2013). RNA in unexpected places: long non-coding RNA functions in diverse cellular contexts. Nat. Rev. Mol. Cell Biol. *14*, 699–712.

10. E, S., Costa, M.C., Kurc, S., Drozdz, A., Cortez-Dias, N., and Enguita, F.J. (2018). The circulating non-coding RNA landscape for biomarker research: lessons and prospects from cardiovascular diseases. Acta. Pharmacol. Sin. *39*, 1085–1099.

11. Chen, W.M., Huang, M.D., Kong, R., Xu, T.P., Zhang, E.B., Xia, R., Sun, M., De, W., and Shu, Y.Q. (2015). Antisense Long Noncoding RNA HIF1A-AS2 Is Upregulated in Gastric Cancer and Associated with Poor Prognosis. Dig. Dis. Sci. *60*, 1655–1662.

12. Chen, M., Zhuang, C., Liu, Y., Li, J., Dai, F., Xia, M., Zhan, Y., Lin, J., Chen, Z., He, A., et al. (2016). Tetracycline-inducible shRNA targeting antisense long non-coding RNA HIF1A-AS2 represses the malignant phenotypes of bladder cancer. Cancer Lett. *376*, 155–164.

13. Lin, J., Shi, Z., Yu, Z., and He, Z. (2018). LncRNA HIF1A-AS2 positively affects the progression and EMT formation of colorectal cancer through regulating miR-129-5p and DNMT3A. Biomed. Pharmacother. *98*, 433–439.

14. Mineo, M., Ricklefs, F., Rooj, A.K., Lyons, S.M., Ivanov, P., Ansari, K.I., Nakano, I., Chiocca, E.A., Godlewski, J., and Bronisz, A. (2016). The Long Non-coding RNA HIF1A-AS2 Facilitates the Maintenance of Mesenchymal Glioblastoma Stem-like Cells in Hypoxic Niches. Cell Rep. *15*, 2500–2509.

15. Durbas, M., Horwacik, I., Boratyn, E., and Rokita, H. (2016). Downregulation of the PHLDA1 gene in IMR-32 neuroblastoma cells increases levels of Aurora A, TRKB and affects proteins involved in apoptosis and autophagy pathways. Int. J. Oncol. *49*, 823–837.

16. Toyoshima, Y., Karas, M., Yakar, S., Dupont, J., Lee Helman, and LeRoith, D. (2004). TDAG51 mediates the effects of insulin-like growth factor I (IGF-I) on cell survival. J. Biol. Chem. *279*, 25898–25904.

17. Park, C.G., Lee, S.Y., Kandala, G., Lee, S.Y., and Choi, Y. (1996). A novel gene product that couples TCR signaling to Fas(CD95) expression in activation-induced cell death. Immunity *4*, 583–591.

18. Duquette, M.L., Kim, J., Shi, L.Z., and Berns, M.W. (2018). LSD1 mediated changes in the local redox environment during the DNA damage response. PLoS ONE *13*, e0201907.

19. Ambrosio, S., Amente, S., Saccà, C.D., Capasso, M., Calogero, R.A., Lania, L., and Majello, B. (2017). LSD1 mediates MYCN control of epithelial-mesenchymal

transition through silencing of metastatic suppressor NDRG1 gene. Oncotarget *8*, 3854–3869.

20. Mansoori, Z., Ghaedi, H., Sadatamini, M., Vahabpour, R., Rahimipour, A., Shanaki, M., Saeidi, L., and Kazerouni, F. (2018). Downregulation of long non-coding RNAs LINC00523 and LINC00994 in type 2 diabetes in an Iranian cohort. Mol. Biol. Rep. *45*, 1227–1233.

21. Zampetaki, A., Albrecht, A., and Steinhofel, K. (2018). Long Non-coding RNA Structure and Function: Is There a Link? Front. Physiol. *9*, 1201.

22. Ferretti, C., Bruni, L., Dangles-Marie, V., Pecking, A.P., and Bellet, D. (2007). Molecular circuits shared by placental and cancer cells, and their implications in the proliferative, invasive and migratory capacities of trophoblasts. Hum. Reprod. Update *13*, 121–141.

23. Holtan, S.G., Creedon, D.J., Haluska, P., and Markovic, S.N. (2009). Cancer and pregnancy: parallels in growth, invasion, and immune modulation and implications for cancer therapeutic agents. Mayo Clin. Proc. *84*, 985–1000.

24. Esteve-Valverde, E., Ferrer-Oliveras, R., Gil-Aliberas, N., Baraldès-Farré, A., Llurba, E., and Alijotas-Reig, J. (2018). Pravastatin for Preventing and Treating Preeclampsia: A Systematic Review. Obstet. Gynecol. Surv. *73*, 40–55.

25. Janani, F., and Changaee, F. (2017). Seasonal variation in the prevalence of preeclampsia. J. Family Med. Prim. Care *6*, 766–769.

26. Lyall, F., Robson, S.C., and Bulmer, J.N. (2013). Spiral artery remodeling and trophoblast invasion in preeclampsia and fetal growth restriction: relationship to clinical outcome. Hypertension *62*, 1046–1054.

27. Kuske, M.D., and Johnson, J.P. (2000). Assignment of the human PHLDA1 gene to chromosome 12q15 by radiation hybrid mapping. Cytogenet. Cell Genet. *89*, 1.

28. Moad, A.I., Muhammad, T.S., Oon, C.E., and Tan, M.L. (2013). Rapamycin induces apoptosis when autophagy is inhibited in T-47D mammary cells and both processes are regulated by Phlda1. Cell Biochem. Biophys. *66*, 567–587.

29. Sellheyer, K., and Nelson, P. (2011). Follicular stem cell marker PHLDA1 (TDAG51) is superior to cytokeratin-20 in differentiating between trichoepithelioma and basal cell carcinoma in small biopsy specimens. J. Cutan. Pathol. *38*, 542–550.

30. Johnson, E.O., Chang, K.H., de Pablo, Y., Ghosh, S., Mehta, R., Badve, S., and Shah, K. (2011). PHLDA1 is a crucial negative regulator and effector of Aurora A kinase in breast cancer. J. Cell Sci. *124*, 2711–2722.

31. Fearon, A.E., Carter, E.P., Clayton, N.S., Wilkes, E.H., Baker, A.M., Kapitonova, E., Bakhouche, B.A., Tanner, Y., Wang, J., Gadaleta, E., et al. (2018). PHLDA1 Mediates Drug Resistance in Receptor Tyrosine Kinase-Driven Cancer. Cell Rep. *22*, 2469–2481.

32. Marchiori, A.C., Casolari, D.A., and Nagai, M.A. (2008). Transcriptional up-regulation of PHLDA1 by 17beta-estradiol in MCF-7 breast cancer cells. Braz. J. Med. Biol. Res. *41*, 579–582.

33. Nagai, M.A. (2016). Pleckstrin homology-like domain, family A, member 1 (*PHLDA1*) and cancer. Biomed. Rep. *4*, 275–281.

OMTN, Volume *16*

Supplemental Information

lncRNA HIF1A Antisense RNA 2 Modulates Trophoblast Cell Invasion and Proliferation through Upregulating PHLDA1 Expression

Dan Wu, Nana Yang, Yetao Xu, Sailan Wang, Yuanyuan Zhang, Matthew Sagnelli, Bingqing Hui, Zhenyao Huang, and Lizhou Sun

Supplemental Tables

Table S1 qRT-PCR and oligonucleotide.

qPCR sequences	
PHLDA1	F: TGCCTGAAAGGGGCAGCTCC
	R: TGATCTGGTGCGGGGCGGA
TFPI2	F: GCTGTCGATTCTGCTGCTTT
	R: CAAGCCTCCCAGGTGTAGAA
RND3	F: AAAGAATAGAGTTGAGCCTGTGG
	R: AAGAGCATTTTGGTATTTGGACA
GEM	F: CTCAATCACAGACCGAGCGA
	R: TTGGCTCTGCTCCTCTTACC
SPRY2	F: GCGATCACGGAGTTCAG
	R: GTGGAGTCTCTCGTGT
ADAM19	F: CACTCCGAGAATGCCATTGG
	R: TCCCTCCTGTTGCATCCATT
SIK1	F: CCACACGGCAGGTTATCTC
	R: GACCTACGCCCCACACATCT
DUSP5	F: CCGACCCACCTACACTACAAA
	R: GTAGCTTCCATCAGGGCATCA
SPRY4	F: CCAGGATGTCACCCACCATTG
	R: TGTGCTGCTGCTGCTC
ERRFI1	F: CGCTGTGATTGCTCTTCGCT

	R: GGAGGACAAGCTAACCCGAAT
siRNA Oligonucleotide	
si-HIF-1#	5'-GGCUCUGGCACUUCCUACAUAAUUU-3'
si-HIF-2#	5'-GGGAACAGAUUAGAAAUCUUCAGAG-3'
si-HIF-3#	5'-GACUAUAAUGCUGAGAACUGCUUCA-3'
si-PHLDA1-1#	5'-UGCAGUACAAGAAUCGUCAGGCCAU-3'
si-PHLDA1-2#	5'-CCUUCAGUGAGCGCUCGCAAGAGGA-3'
si-PHLDA1-3#	5'-UGCCUCCUGCGUGUUAGCCUCCUCU-3'
primers of NCALD promotor regions	
PHLDA1	1F: GGCTAGGTCTCGGTTATGCC
	1R: AATGCAATACCCCCAGCTCC
	2F: AGAAGAAAGCCGAAGACGGG
	2R: TTCCCACGCATATTCGCTCA
	3F: CCCGGGCTAATTCCCAAGAA
	3R: CTCAGAAAGTGAGGACGGGG
	4F: TGAGCGAATATGCGTGGGAA
	4R: CCGGACGCCTAGGTAAACAA
TFPI2	1F: GCCTTTGAGGATTCTGGGGG
	1R: GGCTACATGGGAGACGAAGG
	2F: TTTGAGGATTCTGGGGGCTC

	2R: GGGAGACGAAGGGAGCAAAT
	3F: CTTTGAGGATTCTGGGGGCTC
	3R: TGGGAGACGAAGGGAGCAAA
	4F: AGAGCCTTTGAGGATTCTGGG
	4R: TTGGCTACATGGGAGACGAAG
SPRY2	1F: GAGAAGTCAGGGTGAGACCG
	1R: TGCTTCACTCGTCCAGCTTT
	2F: CTTTTGAATGCCTCCTGCGG
	2R: ACAGAGCAGTTGTTGTCCCA
	3F: GGACGAGTGAAGCACCATGT
	3R: GTGGGAGCACCAGTGGAAAA

Probe of FISH

LncRNA HIF1A-AS2	5’-FAM- augagugaagcaguucucagcauuauaguc-3’

Table S2 Analysis of the RNA transcriptome sequencing data.

GeneID	NC Expression	HIF1AAS2 Expression	log2FoldChange HIF1AAS2/NC	FDR	Up/Down RegulationHIF1AAS2/NC	P value	Symbol
8293	0.01	6.74	9.396604781	3.77E-28	Up	7.97E-30	SERF1A
100861437	0.01	5.86	9.194756854	4.29E-10	Up	2.95E-11	NARR
8710	0.01	4.36	8.768184325	2.59E-21	Up	7.32E-23	SERPINB7
3885	0.01	4.33	8.758223215	4.80E-16	Up	1.91E-17	KRT34

692094	0.01	4.18	8.707359132	4.45E-06	Up	5.31E-07	MSMP
4207	0.01	2.05	7.6794801	1.25E-08	Up	1.04E-09	BORCS8-MEF2B
4322	0.01	1.88	7.554588852	3.30E-11	Up	2.04E-12	MMP13
414060	0.01	1.59	7.312882955	3.63E-07	Up	3.67E-08	TBC1D3C
729877	0.01	1.18	6.882643049	2.33E-05	Up	3.15E-06	TBC1D3H
100128553	0.01	1.08	6.754887502	4.45E-06	Up	5.31E-07	CTAGE4
107986353	0.01	0.93	6.539158811	3.63E-07	Up	3.67E-08	LOC107986353
150221	0.01	0.7	6.129283017	5.44E-09	Up	4.27E-10	RIMBP3C
100526740	0.02	1.38	6.108524457	2.14E-15	Up	9.03E-17	ATP5J2-PTCD1
4314	0.19	12.74	6.067222049	2.22E-48	Up	2.43E-50	MMP3
441430	0.01	0.66	6.044394119	0.000619299	Up	0.00011112	ANKRD20A2
102725035	0.01	0.59	5.882643049	0.000619512	Up	0.00011112	LOC102725035
23117	0.01	0.59	5.882643049	0.000121207	Up	1.87E-05	NPIPB3
4312	0.44	22.62	5.683951595	7.16E-92	Up	3.09E-94	MMP1
127294	0.01	0.5	5.64385619	1.94E-06	Up	2.18E-07	MYOM3
145781	0.01	0.49	5.614709844	1.02E-05	Up	1.29E-06	GCOM1
3598	0.09	3.15	5.129283017	3.30E-08	Up	2.86E-09	IL13RA2
11009	0.99	28.57	4.850928701	5.83E-96	Up	2.34E-98	IL24
23617	0.04	1.08	4.754887502	0.000275341	Up	4.56E-05	TSSK2
5055	0.25	6.54	4.709290636	3.09E-22	Up	8.47E-24	SERPINB2
5801	0.13	2.84	4.449307401	5.50E-13	Up	2.90E-14	PTPRR
150094	0.14	2.93	4.387401932	4.25E-24	Up	1.05E-25	SIK1

25907	1.28	23.41	4.192909219	1.07E-71	Up	6.79E-74	TMEM158
55567	0.04	0.73	4.189824559	2.41E-08	Up	2.05E-09	DNAH3
6123	0.08	1.25	3.965784285	0.000412218	Up	7.11E-05	RPL3L
114960	0.08	1.21	3.918863237	0.000193135	Up	3.10E-05	TSGA13
27063	1.14	16.74	3.876193798	2.38E-51	Up	2.37E-53	ANKRD1
7980	21.82	281.28	3.688283969	0	Up	0	TFPI2
3814	1.18	15.07	3.674820652	6.84E-16	Up	2.73E-17	KISS1
51129	1.34	15.45	3.527301932	4.03E-42	Up	5.32E-44	ANGPTL4
4600	0.06	0.69	3.523561956	0.000875663	Up	0.000162144	MX2
316	0.87	8.99	3.36923381	2.31E-60	Up	1.86E-62	AOX1
100134938	0.7	7.17	3.356546292	6.20E-14	Up	2.99E-15	UPK3BL1
50486	4.49	43.93	3.290419149	4.14E-56	Up	3.55E-58	G0S2
58538	0.3	2.84	3.242856524	8.38E-09	Up	6.79E-10	MPP4
11262	0.29	2.56	3.142019005	4.80E-05	Up	6.87E-06	SP140
57214	1.08	9.53	3.141444902	1.40E-87	Up	6.49E-90	CEMIP
56137	0.05	0.42	3.070389328	0.000412071	Up	7.11E-05	PCDHA12
136332	0.13	1.09	3.067744607	9.74E-05	Up	1.47E-05	LRGUK
654	0.16	1.31	3.033423002	2.14E-05	Up	2.88E-06	BMP6
7185	0.51	4.13	3.017572629	1.37E-22	Up	3.68E-24	TRAF1
57016	0.19	1.52	3	0.000877185	Up	0.000162048	AKR1B10
202658	0.37	2.94	2.990218979	2.62E-06	Up	3.02E-07	TRIM39-RPP21
390	38.53	305.25	2.985937204	0	Up	0	RND3

4907	1.51	11.84	2.971048626	1.08E-58	Up	9.02E-61	NT5E
11082	0.8	6.17	2.947198584	1.22E-15	Up	5.05E-17	ESM1
23643	0.66	4.76	2.850423644	0.000761873	Up	0.000139475	LY96
64078	0.1	0.71	2.827819025	0.000321082	Up	5.40E-05	SLC28A3
116211	1.66	11.58	2.802380107	1.97E-14	Up	9.02E-16	TM4SF19
7111	0.13	0.9	2.791413378	0.000387835	Up	6.64E-05	TMOD1
100861412	0.2	1.35	2.754887502	2.02E-08	Up	1.71E-09	FSBP
2919	0.64	4.26	2.73470962	7.69E-06	Up	9.54E-07	CXCL1
10468	0.96	6.22	2.695808269	1.14E-16	Up	4.34E-18	FST
54206	8.68	55.03	2.664451381	3.36E-182	Up	4.36E-185	ERRFI1
6446	10.16	59.88	2.559173819	5.77E-148	Up	1.21E-150	SGK1
3576	6.29	37.06	2.558730959	1.46E-64	Up	1.06E-66	CXCL8
3371	0.29	1.69	2.542898441	2.66E-12	Up	1.49E-13	TNC
9510	1.65	9.44	2.516320835	1.53E-44	Up	1.84E-46	ADAMTS1
5054	11.79	64.91	2.460877038	1.72E-198	Up	1.80E-201	SERPINE1
107986876	0.24	1.32	2.459431619	0.000475476	Up	8.32E-05	LOC107986876
1827	18.74	102.05	2.445083324	7.43E-252	Up	4.59E-255	RCAN1
114801	0.64	3.4	2.409390936	1.40E-10	Up	9.22E-12	TMEM200A
7078	7.73	40.84	2.401442547	9.67E-214	Up	8.36E-217	TIMP3
8325	1.46	7.56	2.372417865	8.23E-23	Up	2.16E-24	FZD8

283518	0.46	2.37	2.365181293	0.00035774	Up	6.07E-05	KCNRG
4929	0.23	1.17	2.346802764	4.20E-05	Up	5.92E-06	NR4A2
1305	1.01	5.12	2.341788517	2.57E-14	Up	1.19E-15	COL13A1
92949	0.19	0.95	2.321928095	0.00065551	Up	0.000118386	ADAMTSL1
8214	1.31	6.45	2.299732349	1.26E-07	Up	1.19E-08	DGCR6
2669	1.17	5.71	2.286982216	2.33E-11	Up	1.42E-12	GEM
11343	0.53	2.54	2.260764232	2.67E-08	Up	2.28E-09	MGLL
768	1	4.76	2.250961574	5.79E-07	Up	6.05E-08	CA9
5649	0.36	1.64	2.187627003	1.33E-16	Up	5.09E-18	RELN
140456	0.48	2.08	2.115477217	3.87E-05	Up	5.43E-06	ASB11
2827	0.5	2.16	2.111031312	0.000243484	Up	3.99E-05	GPR3
2246	0.51	2.18	2.095758983	6.84E-07	Up	7.25E-08	FGF1
10326	1.16	4.82	2.054908341	6.82E-09	Up	5.47E-10	SIRPB1
9201	0.76	3.07	2.014167332	9.26E-17	Up	3.50E-18	DCLK1
1847	6.46	25.92	2.004459648	1.67E-49	Up	1.76E-51	DUSP5
81848	0.7	2.8	2	6.28E-11	Up	3.97E-12	SPRY4
114907	1.08	4.32	2	1.78E-22	Up	4.82E-24	FBXO32
4071	36.39	143.73	1.981747263	4.56E-180	Up	6.18E-183	TM4SF1
3592	0.83	3.23	1.960350923	0.00052092	Up	9.21E-05	IL12A
10253	3.19	12.36	1.954050414	2.96E-20	Up	9.03E-22	SPRY2
26585	1.86	7.12	1.93657462	3.24E-21	Up	9.18E-23	GREM1
11199	3.82	14.49	1.923413052	5.12E-15	Up	2.24E-16	ANXA10

85450	1.79	6.77	1.919196246	2.03E-32	Up	3.64E-34	ITPRIP
26872	1.14	4.31	1.918654045	8.41E-05	Up	1.26E-05	STEAP1
9732	0.59	2.23	1.918256851	1.88E-12	Up	1.03E-13	DOCK4
64859	13.29	50	1.91158699	6.05E-111	Up	2.02E-113	NABP1
101928841	0.27	1	1.888968688	8.70E-07	Up	9.33E-08	LOC101928841
6422	12.58	45.82	1.864845536	4.48E-140	Up	9.94E-143	SFRP1
1839	6.72	24.28	1.853235283	4.88E-39	Up	7.11E-41	HBEGF
56911	6.86	24.67	1.846477234	2.32E-29	Up	4.64E-31	MAP3K7CL
2921	1.12	4.02	1.843696769	0.000899748	Up	0.000167048	CXCL3
23645	20.99	74.85	1.83430015	7.40E-119	Up	2.10E-121	PPP1R15A
9734	2.75	9.76	1.827449529	2.57E-20	Up	7.79E-22	HDAC9
3914	9.03	32.03	1.826625905	6.41E-90	Up	2.81E-92	LAMB3
10397	18.76	64.05	1.771538743	7.45E-128	Up	1.93E-130	NDRG1
26191	1.49	5.08	1.769516166	9.70E-08	Up	9.03E-09	PTPN22
10202	3.83	12.89	1.750835966	1.54E-13	Up	7.69E-15	DHRS2
79875	0.36	1.21	1.748938236	2.08E-07	Up	2.03E-08	THSD4
1846	0.67	2.25	1.747692001	1.62E-08	Up	1.35E-09	DUSP4
9518	19.55	65.2	1.737703357	3.39E-48	Up	3.73E-50	GDF15
728689	4.08	13.47	1.723108793	2.77E-17	Up	1.01E-18	EIF3CL
100533467	0.91	3	1.72102405	6.65E-10	Up	4.69E-11	BIVM-ERCC5

5606	14.7	48.17	1.712318769	1.50E-65	Up	1.07E-67	MAP2K3
5362	0.56	1.83	1.708344916	1.36E-08	Up	1.13E-09	PLXNA2
5997	3.51	11.35	1.693149362	1.25E-09	Up	9.15E-11	RGS2
1848	4.65	14.99	1.688697762	2.83E-30	Up	5.41E-32	DUSP6
22822	19.63	63.2	1.686864386	2.34E-221	Up	1.88E-224	PHLDA1
7424	3.81	12.26	1.686096076	1.71E-15	Up	7.13E-17	VEGFC
5327	4.52	14.27	1.658590657	2.16E-27	Up	4.68E-29	PLAT
5329	24.71	77.73	1.653376506	3.56E-56	Up	3.03E-58	PLAUR
135	1.72	5.36	1.639824436	1.16E-07	Up	1.09E-08	ADORA2A
58489	2.72	8.47	1.638755318	6.11E-12	Up	3.53E-13	ABHD17C
129303	1.68	5.21	1.632822139	2.54E-05	Up	3.46E-06	TMEM150A
50649	1.35	4.18	1.630543535	0.000247875	Up	4.07E-05	ARHGEF4
7730	1.33	4.1	1.624197664	3.77E-06	Up	4.44E-07	ZNF177
8482	1.52	4.65	1.613159393	1.57E-09	Up	1.17E-10	SEMA7A
4502	67.91	207.71	1.612874738	5.48E-50	Up	5.65E-52	MT2A
79669	2.08	6.36	1.612443237	7.01E-08	Up	6.38E-09	C3orf52
6809	15.63	47.62	1.607249842	7.19E-64	Up	5.32E-66	STX3
2012	16.3	49.43	1.600514942	1.39E-75	Up	7.98E-78	EMP1
837	38.75	115.73	1.578494679	2.25E-80	Up	1.19E-82	CASP4
2297	4.38	12.97	1.566175705	7.80E-16	Up	3.15E-17	FOXD1
50515	1.64	4.84	1.561311233	4.07E-15	Up	1.75E-16	CHST11
22934	4.58	13.43	1.552039801	3.24E-13	Up	1.68E-14	RPIA
10105	41.52	121.53	1.549434142	8.24E-115	Up	2.49E-11	PPIF

8793	15.11	44.04	1.543310808	1.85E-81	Up	9.49E-84	TNFRSF10D
57476	3.42	9.85	1.526127399	2.85E-36	Up	4.59E-38	GRAMD1B
8942	3.28	9.27	1.498873524	6.28E-09	Up	4.99E-10	KYNU
51175	4.18	11.79	1.495988871	1.21E-13	Up	5.95E-15	TUBE1
90874	2.79	7.86	1.49426419	1.57E-19	Up	4.98E-21	ZNF697
10007	38.74	108.8	1.489782698	9.77E-122	Up	2.71E-124	GNPDA1
7128	1.31	3.66	1.482276837	5.87E-09	Up	4.63E-10	TNFAIP3
4783	2.82	7.87	1.480668473	7.37E-09	Up	5.92E-10	NFIL3
83931	7.27	19.89	1.452016007	8.34E-35	Up	1.41E-36	STK40
57522	2.79	7.58	1.441932726	1.17E-18	Up	3.94E-20	SRGAP1
91	4.12	11.12	1.432440546	4.99E-11	Up	3.12E-12	ACVR1B
3976	3.12	8.42	1.432274204	9.46E-16	Up	3.85E-17	LIF
123	11.77	31.62	1.425723047	1.88E-28	Up	3.90E-30	PLIN2
134637	2.79	7.45	1.416975304	7.58E-05	Up	1.12E-05	ADAT2
6533	3.58	9.5	1.407967926	1.87E-20	Up	5.65E-22	SLC6A6
160760	1.27	3.37	1.407920094	2.53E-06	Up	2.91E-07	PPTC7
4097	7.61	20.05	1.397633878	1.04E-44	Up	1.24E-46	MAFG
8061	13.99	36.7	1.391384101	1.07E-27	Up	2.29E-29	FOSL1
6875	2.29	6	1.389614902	1.12E-07	Up	1.05E-08	TAF4B
102724159	4.94	12.92	1.387023123	3.09E-19	Up	9.99E-21	LOC102724159
3678	36.5	95.18	1.382761991	4.35E-178	Up	6.17E-181	ITGA5

25890	2.82	7.35	1.382049087	1.92E-15	Up	8.04E-17	ABI3BP
10068	1.39	3.62	1.380904814	0.000287568	Up	4.78E-05	IL18BP
55691	2.46	6.4	1.37941359	4.56E-14	Up	2.17E-15	FRMD4A
28951	1.16	3.01	1.375638682	1.94E-06	Up	2.17E-07	TRIB2
114880	0.49	1.27	1.373974843	0.000106611	Up	1.63E-05	OSBPL6
3673	2.54	6.47	1.348937215	5.88E-22	Up	1.63E-23	ITGA2
64147	1.28	3.26	1.348728154	0.000431648	Up	7.49E-05	KIF9
153222	3.57	9.06	1.343586976	4.03E-16	Up	1.59E-17	CREBRF
8660	0.66	1.67	1.339310173	1.37E-05	Up	1.78E-06	IRS2
92737	1.92	4.8	1.321928095	5.46E-07	Up	5.67E-08	DNER
9353	1.87	4.67	1.32038428	7.37E-17	Up	2.77E-18	SLIT2
9903	4.97	12.41	1.320185359	8.35E-24	Up	2.09E-25	KLHL21
4609	31	76.78	1.308462345	4.33E-73	Up	2.65E-75	MYC
23764	11.17	27.51	1.300326954	7.50E-27	Up	1.67E-28	MAFF
5270	40.96	100.66	1.297202882	8.99E-88	Up	4.05E-90	SERPINE2
101060226	3.26	8.01	1.296930278	1.57E-12	Up	8.58E-14	NBPF19
206358	2.2	5.4	1.295455884	1.78E-06	Up	1.99E-07	SLC36A1
8496	24.62	60.22	1.290411946	2.26E-138	Up	5.31E-141	PPFIBP1
55966	4.01	9.76	1.283278911	2.78E-17	Up	1.02E-18	AJAP1
26018	2.54	6.16	1.278101854	5.51E-13	Up	2.91E-14	LRIG1
9907	5.88	14.26	1.278085922	6.97E-17	Up	2.62E-18	AP5Z1
28996	0.43	1.04	1.274174963	9.19E-07	Up	9.89E-08	HIPK2
2118	4.69	11.33	1.272488033	9.82E-11	Up	6.38E-12	ETV4

7052	10.84	26.15	1.27044619	2.16E-46	Up	2.45E-48	TGM2
127262	5.43	13.09	1.269440994	1.32E-12	Up	7.16E-14	TPRG1L
285704	9.31	22.43	1.268576548	6.43E-36	Up	1.05E-37	RGMB
2290	2.7	6.48	1.263034406	1.76E-08	Up	1.47E-09	FOXG1
10370	37.45	89.74	1.260785465	1.44E-65	Up	1.01E-67	CITED2
89795	13.01	30.99	1.252181793	3.50E-113	Up	1.12E-115	NAV3
11259	2.1	5	1.251538767	5.09E-06	Up	6.14E-07	FILIP1L
64093	2.88	6.84	1.247927513	4.96E-10	Up	3.45E-11	SMOC1
2294	2.04	4.83	1.243454037	3.72E-05	Up	5.21E-06	FOXF1
1288	0.98	2.32	1.243271151	6.34E-06	Up	7.79E-07	COL4A6
10123	4.53	10.71	1.241375525	2.51E-16	Up	9.77E-18	ARL4C
9955	2.96	6.99	1.23969528	3.07E-11	Up	1.89E-12	HS3ST3A1
57613	4.67	11.02	1.238629769	1.17E-19	Up	3.69E-21	FAM234B
55076	9.48	22.07	1.219127665	4.32E-13	Up	2.26E-14	TMEM45A
4254	5.55	12.92	1.219046393	9.17E-26	Up	2.13E-27	KITLG
414189	3.54	8.23	1.21714307	4.69E-07	Up	4.81E-08	AGAP6
220213	2.28	5.3	1.216958535	1.54E-06	Up	1.71E-07	OTUD1
8728	5.32	12.34	1.213844244	2.45E-31	Up	4.53E-33	ADAM19
64782	17.33	40.12	1.211049951	2.06E-47	Up	2.30E-49	AEN
25822	4.72	10.9	1.20746937	5.94E-10	Up	4.16E-11	DNAJB5
80045	3.33	7.68	1.205584134	1.71E-05	Up	2.25E-06	GPR157
9792	2.04	4.7	1.204091605	8.43E-10	Up	6.01E-11	SERTAD2
57666	0.95	2.18	1.198328716	0.000737445	Up	0.000134	FBRSL1

29057	4.93	11.31	1.197939378	2.35E-10	Up	1.58E-11	FAM156A
599	4.98	11.41	1.196081144	1.27E-14	Up	5.76E-16	BCL2L2
81606	1.45	3.32	1.195130341	0.000330948	Up	5.58E-05	LBH
148641	1.22	2.79	1.193383974	0.000979468	Up	0.000183964	SLC35F3
91373	3.43	7.84	1.192645078	8.07E-08	Up	7.41E-09	UAP1L1
57478	4.7	10.7	1.186878135	1.03E-11	Up	6.08E-13	USP31
85414	2.61	5.94	1.186413124	7.74E-09	Up	6.24E-10	SLC45A3
54972	6.54	14.82	1.180182907	8.89E-19	Up	2.93E-20	TMEM132A
115123	3.83	8.67	1.178687601	1.66E-07	Up	1.61E-08	3-Mar
1026	97.32	219.98	1.176564138	7.44E-163	Up	1.24E-165	CDKN1A
100101267	1	2.25	1.169925001	4.13E-05	Up	5.82E-06	POM121C
868	3.65	8.2	1.167727446	1.13E-10	Up	7.36E-12	CBLB
5874	1.5	3.36	1.163498732	0.000218097	Up	3.54E-05	RAB27B
440138	1.87	4.18	1.160464672	0.000242269	Up	3.97E-05	ALG11
220323	4.96	11.08	1.159545856	1.02E-07	Up	9.49E-09	OAF
3589	25.01	55.77	1.156984213	1.33E-43	Up	1.70E-45	IL11
9945	13.27	29.55	1.15498976	1.27E-31	Up	2.31E-33	GFPT2
284217	8.1	18.03	1.154405584	4.74E-54	Up	4.33E-56	LAMA1
7975	6.38	14.2	1.154262601	4.33E-13	Up	2.27E-14	MAFK
57192	2.37	5.27	1.152915903	0.000249583	Up	4.10E-05	MCOLN1
11221	2.62	5.82	1.151452341	1.05E-05	Up	1.32E-06	DUSP10

285761	6.17	13.69	1.149780052	1.24E-08	Up	1.03E-09	DCBLD1
23119	3.01	6.66	1.14575869	4.02E-16	Up	1.58E-17	HIC2
64866	1.45	3.19	1.137503524	3.23E-05	Up	4.47E-06	CDCP1
898	9.25	20.29	1.133243594	2.61E-12	Up	1.46E-13	CCNE1
8744	6.24	13.67	1.131395309	7.55E-08	Up	6.90E-09	TNFSF9
25977	10.04	21.94	1.127804256	2.30E-18	Up	7.86E-20	NECAP1
80380	2.37	5.16	1.122484007	0.000126244	Up	1.96E-05	PDCD1LG2
80005	4.99	10.86	1.121912382	5.18E-08	Up	4.62E-09	DOCK5
9223	0.91	1.98	1.12156198	6.64E-06	Up	8.16E-07	MAGI1
24147	6.17	13.37	1.115657071	1.11E-11	Up	6.53E-13	FJX1
7088	6.81	14.75	1.114988251	1.83E-18	Up	6.23E-20	TLE1
23409	41.34	89.42	1.113059157	2.27E-38	Up	3.41E-40	SIRT4
5128	19.9	42.99	1.11123268	5.69E-55	Up	5.02E-57	CDK17
2745	23.39	50.16	1.100645486	1.00E-17	Up	3.53E-19	GLRX
5163	7.74	16.53	1.094681253	1.06E-15	Up	4.38E-17	PDK1
28231	27.26	58.12	1.092249141	2.14E-50	Up	2.16E-52	SLCO4A1
7832	6.44	13.73	1.092199032	1.16E-11	Up	6.88E-13	BTG2
7022	2.01	4.25	1.08026734	0.000264239	Up	4.36E-05	TFAP2C
2034	3.58	7.55	1.076517057	5.86E-12	Up	3.37E-13	EPAS1
3575	10.59	22.26	1.071751003	1.22E-29	Up	2.40E-31	IL7R
5209	10.48	22.02	1.071175752	1.12E-24	Up	2.70E-26	PFKFB3
4651	7.38	15.5	1.070575494	4.79E-39	Up	6.95E-41	MYO10
94081	49.84	104.63	1.069920594	6.07E-62	Up	4.64E-64	SFXN1

388	45.24	94.92	1.069113171	1.91E-65	Up	1.37E-67	RHOB
11174	9.23	19.36	1.0686764	6.79E-19	Up	2.23E-20	ADAMTS6
2114	4.79	10.04	1.067661708	8.47E-12	Up	4.95E-13	ETS2
55238	20.71	43.39	1.067035033	1.74E-26	Up	3.91E-28	SLC38A7
9842	11.54	24.16	1.065977231	1.51E-31	Up	2.77E-33	PLEKHM1
64750	20.39	42.67	1.065360335	6.83E-49	Up	7.33E-51	SMURF2
123879	3.35	7.01	1.065253349	7.01E-13	Up	3.73E-14	DCUN1D3
1051	26.64	55.69	1.06382421	7.33E-34	Up	1.26E-35	CEBPB
83985	13.64	28.49	1.062611977	8.24E-18	Up	2.90E-19	SPNS1
2119	7.23	15.04	1.056737015	5.77E-18	Up	2.01E-19	ETV5
1604	20.12	41.84	1.056252546	9.40E-28	Up	2.00E-29	CD55
54984	7.42	15.43	1.05624697	6.72E-07	Up	7.11E-08	PINX1
330	14.88	30.93	1.055632307	1.23E-41	Up	1.64E-43	BIRC3
2004	5.18	10.76	1.054654075	4.92E-13	Up	2.59E-14	ELK3
3491	24.5	50.85	1.053466025	4.53E-33	Up	7.94E-35	CYR61
11153	4.29	8.89	1.051205771	9.29E-05	Up	1.40E-05	FICD
11217	10.73	22.18	1.047609289	1.81E-44	Up	2.18E-46	AKAP2
1611	7.25	14.96	1.045057275	2.07E-10	Up	1.38E-11	DAP
342184	2.68	5.48	1.031942893	4.01E-21	Up	1.15E-22	FMN1
1951	1.1	2.24	1.025995209	8.16E-08	Up	7.51E-09	CELSR3
283820	11.54	23.37	1.01801451	1.53E-28	Up	3.15E-30	NOMO2
9953	1.62	3.28	1.017702002	1.14E-05	Up	1.44E-06	HS3ST3B1
1843	18.53	37.51	1.017412382	1.27E-20	Up	3.81E-22	DUSP1

3437	3.48	7.04	1.016488123	1.60E-05	Up	2.10E-06	IFIT3
115708	7.55	15.26	1.015206413	1.17E-13	Up	5.76E-15	TRMT61A
11334	22.74	45.95	1.014832607	6.23E-21	Up	1.82E-22	TUSC2
84879	3.75	7.57	1.013402705	3.23E-05	Up	4.48E-06	MFSD2A
26064	17.38	34.98	1.009102207	4.28E-46	Up	4.88E-48	RAI14
10954	3.58	7.17	1.002013531	0.000369994	Up	6.31E-05	PDIA5
400745	4.25	8.51	1.001696291	1.71E-09	Up	1.27E-10	SH2D5
56652	4.74	9.48	1	1.88E-08	Up	1.59E-09	C10orf2
9915	3.99	7.98	1	3.89E-14	Up	1.84E-15	ARNT2
9825	2.5	5	1	5.48E-06	Up	6.63E-07	SPATA2
102724594	13.06	0.01	-10.35093918	2.21E-23	Down	5.68E-25	U2AF1L5
107985795	3.48	0.01	-8.442943496	7.18E-05	Down	1.06E-05	LOC107985795
728239	2.58	0.01	-8.011227255	2.98E-12	Down	1.68E-13	MAGED4
102723859	2.26	0.01	-7.820178962	7.87E-10	Down	5.60E-11	TBC1D3E
100532731	2.18	0.01	-7.768184325	1.42E-13	Down	7.05E-15	COMMD3-BMI1
101060389	2.06	0.01	-7.686500527	9.61E-09	Down	7.86E-10	LOC101060389
102724994	1.88	0.01	-7.554588852	1.59E-08	Down	1.33E-09	LOC102724994
100302652	1.85	0.01	-7.531381461	8.51E-07	Down	9.12E-08	GPR75-ASB3
102723722	1.48	0.01	-7.209453366	4.39E-05	Down	6.24E-06	LOC102723722
107987464	1.46	0.01	-7.189824559	1.92E-07	Down	1.87E-08	LOC107987464
284040	1.39	0.01	-7.118941073	2.30E-06	Down	2.62E-07	CDRT4
100533105	1.12	0.01	-6.807354922	2.14E-09	Down	1.61E-10	C8orf44-SGK3
445372	0.87	0.01	-6.442943496	1.65E-05	Down	2.17E-06	TRIM6-TRIM34

85376	0.85	0.01	-6.409390936	5.87E-09	Down	4.63E-10	RIMBP3
107986096	0.8	0.01	-6.321928095	0.000116587	Down	1.79E-05	LOC107986096
100996517	0.61	0.01	-5.930737338	2.65E-08	Down	2.26E-09	LOC100996517
117283	1.35	0.07	-4.269460675	1.02E-05	Down	1.29E-06	IP6K3
51302	1.26	0.07	-4.169925001	0.000251746	Down	4.14E-05	CYP39A1
84734	3.02	0.18	-4.068479738	0.000251841	Down	4.14E-05	FAM167B
54065	5.93	0.41	-3.85433629	4.80E-08	Down	4.26E-09	SMIM11A
286464	0.42	0.03	-3.807354922	0.000251935	Down	4.14E-05	CFAP47
339768	0.55	0.04	-3.781359714	0.000616293	Down	0.000110467	ESPNL
143686	0.41	0.04	-3.357552005	2.67E-05	Down	3.65E-06	SESN3
9037	1.67	0.19	-3.135776779	1.30E-22	Down	3.47E-24	SEMA5A
152816	2	0.27	-2.888968688	0.000152408	Down	2.40E-05	C4orf26
54664	14.25	2.01	-2.825694513	2.34E-95	Down	9.53E-98	TMEM106B
1545	0.92	0.13	-2.823122238	2.78E-05	Down	3.82E-06	CYP1B1
9022	4.93	0.71	-2.795696717	0.000307032	Down	5.14E-05	CLIC3
100288695	2.43	0.35	-2.795529487	0.000832592	Down	0.000153552	LIMS4
84448	1.33	0.2	-2.733354341	0.0004236	Down	7.33E-05	ABLIM2
4973	83.36	12.99	-2.681953847	2.21E-206	Down	2.05E-209	OLR1
100529215	5.33	0.84	-2.6656743	6.19E-15	Down	2.73E-16	ZNF559-ZNF177
57124	2.04	0.33	-2.628031223	2.06E-05	Down	2.76E-06	CD248
4232	73.32	12.39	-2.565030598	4.46E-172	Down	6.88E-175	MEST

8344	25.83	4.37	-2.563342459	4.25E-10	Down	2.92E-11	HIST1H2BE
107983947	3.39	0.58	-2.547160468	0.000633132	Down	0.000113915	LOC107983947
374462	1.83	0.32	-2.515699838	5.98E-14	Down	2.88E-15	PTPRQ
169611	1.08	0.19	-2.506959989	1.37E-06	Down	1.50E-07	OLFML2A
114800	12.58	2.43	-2.372103703	1.02E-43	Down	1.29E-45	CCDC85A
1281	33.33	6.5	-2.358309694	3.50E-156	Down	6.48E-159	COL3A1
11346	1.47	0.29	-2.34169135	3.18E-07	Down	3.19E-08	SYNPO
115701	2.48	0.49	-2.339486466	6.91E-14	Down	3.34E-15	ALPK2
642778	1.52	0.31	-2.293731203	0.000359064	Down	6.10E-05	NPIPA3
148398	3.6	0.74	-2.282399731	7.07E-08	Down	6.44E-09	SAMD11
8935	4.49	0.93	-2.271412824	2.20E-15	Down	9.29E-17	SKAP2
152007	34.17	7.13	-2.260756266	6.27E-60	Down	5.10E-62	GLIPR2
3352	2.03	0.43	-2.239071162	4.54E-05	Down	6.47E-06	HTR1D
728498	1.3	0.28	-2.215012891	4.70E-06	Down	5.63E-07	GOLGA8H
3855	2.8	0.61	-2.198545679	0.000945607	Down	0.00017667	KRT7
120	22.31	4.91	-2.183895584	8.24E-77	Down	4.58E-79	ADD3
23308	2.36	0.52	-2.182203331	0.000114571	Down	1.76E-05	ICOSLG
84913	2.76	0.62	-2.154328146	4.92E-09	Down	3.83E-10	ATOH8
6917	137.39	30.89	-2.153065225	1.79E-286	Down	9.96E-290	TCEA1
84709	86.5	19.84	-2.124288107	2.34E-85	Down	1.11E-87	MGARP
100271927	3.93	0.92	-2.094823546	4.53E-09	Down	3.52E-10	RASA4B

9991	17.08	4.14	-2.044605302	3.77E-82	Down	1.91E-84	PTBP3
56918	2.02	0.49	-2.043501639	0.000945919	Down	0.00017667	C2orf83
1756	4.72	1.18	-2	1.22E-20	Down	3.64E-22	DMD
81493	6.33	1.6	-1.984133595	1.01E-15	Down	4.16E-17	SYNC
728741	4.05	1.04	-1.96133838	2.52E-05	Down	3.42E-06	NPIPB6
10935	108.15	28.1	-1.94439163	2.06E-117	Down	5.98E-120	PRDX3
102724788	5.04	1.32	-1.932885804	9.36E-09	Down	7.63E-10	LOC102724788
223117	3.27	0.86	-1.926882071	1.44E-15	Down	5.95E-17	SEMA3D
4091	5.04	1.36	-1.889817082	1.12E-12	Down	6.03E-14	SMAD6
8153	1.83	0.5	-1.871843649	2.87E-05	Down	3.96E-06	RND2
3280	3.43	0.94	-1.867475914	0.000990561	Down	0.000186353	HES1
10085	11.59	3.19	-1.861252237	3.27E-35	Down	5.42E-37	EDIL3
142940	11.73	3.25	-1.85169139	2.76E-25	Down	6.48E-27	TRUB1
81786	23.02	6.45	-1.835516768	1.27E-17	Down	4.54E-19	TRIM7
266727	2.03	0.57	-1.832445903	0.00054657	Down	9.70E-05	MDGA1
57484	3.46	0.98	-1.819918384	1.03E-14	Down	4.62E-16	RNF150
100133941	5.31	1.52	-1.804640537	1.53E-07	Down	1.47E-08	CD24
653	4.08	1.17	-1.802060622	3.64E-06	Down	4.28E-07	BMP5
767558	42.68	12.32	-1.79255792	8.31E-100	Down	3.18E-102	LUZP6
10959	139.54	40.33	-1.790753428	6.53E-177	Down	9.67E-180	TMED2

26994	23.88	6.99	-1.772438476	1.24E-43	Down	1.58E-45	RNF11
170689	1.02	0.3	-1.765534746	0.000535106	Down	9.47E-05	ADAMTS15
4893	38.22	11.27	-1.761840263	2.69E-100	Down	9.97E-103	NRAS
283078	2.37	0.7	-1.759460232	0.000229116	Down	3.74E-05	MKX
10434	80.5	24.1	-1.739955637	2.26E-122	Down	6.13E-125	LYPLA1
6319	173.12	52.51	-1.721108303	0	Down	0	SCD
9127	5.55	1.69	-1.715464525	8.86E-10	Down	6.36E-11	P2RX6
653145	11.72	3.57	-1.71497659	8.95E-13	Down	4.79E-14	ANXA8
2247	36.76	11.36	-1.694173932	1.67E-139	Down	3.81E-142	FGF2
5654	3.08	0.96	-1.68182404	0.000389202	Down	6.66E-05	HTRA1
23376	10.09	3.15	-1.679502441	1.28E-23	Down	3.24E-25	UFL1
79694	4.13	1.29	-1.678770716	2.81E-10	Down	1.90E-11	MANEA
81575	3.19	1.02	-1.644987272	1.40E-08	Down	1.17E-09	APOLD1
7041	9.79	3.14	-1.640544301	9.09E-10	Down	6.55E-11	TGFB1I1
56925	11.47	3.7	-1.632268215	1.49E-06	Down	1.64E-07	LXN
4131	6.16	1.99	-1.63016192	2.43E-39	Down	3.50E-41	MAP1B
51014	47.02	15.25	-1.624465296	1.86E-100	Down	6.77E-103	TMED7
23089	6.03	1.97	-1.613962372	5.02E-21	Down	1.45E-22	PEG10
5318	6.15	2.03	-1.599106683	1.80E-14	Down	8.24E-16	PKP2
11037	3.23	1.07	-1.593923368	1.64E-09	Down	1.22E-10	STON1
214	38.5	12.79	-1.589842182	8.09E-112	Down	2.65E-11	ALCAM

3426	3.99	1.33	-1.584962501	0.00012468	Down	1.93E-05	CFI
3612	9.57	3.2	-1.58044702	9.55E-17	Down	3.62E-18	IMPA1
84680	2.24	0.75	-1.578536232	0.000990886	Down	0.000186353	ACCS
55809	0.83	0.28	-1.567684509	0.000127764	Down	1.98E-05	TRERF1
122060	3.17	1.08	-1.553451528	5.35E-05	Down	7.72E-06	SLAIN1
253832	19.5	6.69	-1.543396008	1.13E-50	Down	1.13E-52	ZDHHC20
192668	2.72	0.94	-1.53287399	0.000416009	Down	7.18E-05	CYS1
85462	1.43	0.5	-1.516015147	2.44E-05	Down	3.30E-06	FHDC1
55740	18.8	6.63	-1.503651886	1.99E-74	Down	1.16E-76	ENAH
10622	12.31	4.35	-1.500743456	1.12E-19	Down	3.52E-21	POLR3G
8359	422.17	149.82	-1.494593835	1.03E-66	Down	7.04E-69	HIST1H4A
55266	20.42	7.26	-1.491941413	1.50E-44	Down	1.79E-46	TMEM19
7058	18.08	6.43	-1.491504035	7.97E-50	Down	8.26E-52	THBS2
84333	6.19	2.21	-1.48589304	6.25E-21	Down	1.83E-22	PCGF5
197021	3.63	1.3	-1.481457925	0.000254043	Down	4.19E-05	LCTL
6443	7.8	2.8	-1.478047297	9.07E-16	Down	3.67E-17	SGCB
23443	11.33	4.08	-1.473506804	6.93E-19	Down	2.28E-20	SLC35A3
56906	5.18	1.87	-1.469913828	2.06E-05	Down	2.76E-06	THAP10
54510	1.74	0.63	-1.465663572	6.72E-05	Down	9.85E-06	PCDH18
3094	355.28	128.65	-1.465505019	1.01E-105	Down	3.54E-108	HINT1
6102	6.08	2.21	-1.460024954	4.88E-11	Down	3.05E-12	RP2

219539	3.02	1.1	-1.457045026	6.71E-05	Down	9.85E-06	YPEL4
5587	5.16	1.88	-1.456638404	3.65E-09	Down	2.81E-10	PRKD1
1031	44.13	16.11	-1.453803253	1.94E-38	Down	2.89E-40	CDKN2C
255783	8.53	3.12	-1.450999712	0.000992513	Down	0.000187026	INAFM1
54961	6.76	2.48	-1.446683126	3.60E-09	Down	2.77E-10	SSH3
10097	44.56	16.36	-1.445576484	1.16E-77	Down	6.37E-80	ACTR2
9415	30.32	11.18	-1.439349565	8.64E-45	Down	1.02E-46	FADS2
10040	14.97	5.53	-1.436722836	2.01E-16	Down	7.75E-18	TOM1L1
3897	5.82	2.15	-1.436682493	1.80E-13	Down	9.05E-15	L1CAM
8294	497.8	184.08	-1.435233342	7.46E-74	Down	4.42E-76	HIST1H4I
3398	8.69	3.22	-1.432295489	8.57E-06	Down	1.07E-06	ID2
286144	4.18	1.55	-1.431234727	2.14E-07	Down	2.10E-08	TRIQK
219654	2.96	1.1	-1.428093652	1.94E-06	Down	2.17E-07	ZCCHC24
6856	15.47	5.75	-1.427839336	9.95E-16	Down	4.08E-17	SYPL1
7108	20.7	7.71	-1.424828002	1.15E-14	Down	5.18E-16	TM7SF2
3077	17.13	6.4	-1.420381341	1.94E-19	Down	6.20E-21	HFE
83463	21.81	8.17	-1.416581786	5.39E-12	Down	3.09E-13	MXD3
2774	1.52	0.57	-1.415037499	0.000254138	Down	4.19E-05	GNAL
158219	5.14	1.93	-1.413167512	1.40E-07	Down	1.33E-08	TTC39B
3955	3.3	1.24	-1.412125904	0.000148166	Down	2.33E-05	LFNG
4781	3.74	1.41	-1.407343107	6.99E-14	Down	3.38E-15	NFIB
3676	4.27	1.61	-1.407175382	1.45E-18	Down	4.90E-20	ITGA4
57181	17.63	6.65	-1.406606229	1.30E-40	Down	1.79E-42	SLC39A10

9530	23.91	9.03	-1.404816237	1.68E-45	Down	1.96E-47	BAG4
284611	6.37	2.41	-1.402260226	9.12E-15	Down	4.08E-16	FAM102B
286410	11.99	4.54	-1.401067456	7.49E-35	Down	1.26E-36	ATP11C
7351	6.86	2.62	-1.388641765	3.24E-05	Down	4.50E-06	UCP2
51200	52.84	20.32	-1.378730064	2.42E-61	Down	1.90E-63	CPA4
23456	17.16	6.6	-1.378511623	2.26E-26	Down	5.11E-28	ABCB10
103344718	2.96	1.14	-1.376563351	2.64E-05	Down	3.61E-06	HOTS
83879	32.38	12.51	-1.372021196	7.77E-35	Down	1.31E-36	CDCA7
4026	6.96	2.7	-1.366127899	2.81E-39	Down	4.06E-41	LPP
57493	7.06	2.74	-1.36549229	2.83E-27	Down	6.19E-29	HEG1
54842	2	0.78	-1.358453971	0.000239324	Down	3.92E-05	MFSD6
8676	2.23	0.87	-1.357956404	7.92E-05	Down	1.18E-05	STX11
122953	25.2	9.85	-1.355228104	9.51E-24	Down	2.39E-25	JDP2
51523	22.69	8.87	-1.355050599	1.03E-23	Down	2.60E-25	CXXC5
139231	12.09	4.74	-1.35085528	6.22E-37	Down	9.67E-39	FAM199X
157567	6.63	2.6	-1.350497247	1.97E-07	Down	1.92E-08	ANKRD46
2736	1.35	0.53	-1.348895142	0.000657748	Down	0.000118831	GLI2
57534	60.86	23.9	-1.348483716	6.96E-146	Down	1.50E-148	MIB1
6674	7.12	2.81	-1.341307111	5.27E-08	Down	4.72E-09	SPAG1
8353	255.17	100.72	-1.341108535	8.60E-44	Down	1.08E-45	HIST1H3E
4325	12.4	4.9	-1.339486466	1.79E-31	Down	3.29E-33	MMP16
221830	11.31	4.47	-1.339252193	1.04E-17	Down	3.68E-19	TWISTNB

8683	158.74	62.93	-1.334845863	1.19E-73	Down	7.11E-76	SRSF9
11007	73.77	29.27	-1.33361149	1.66E-36	Down	2.64E-38	CCDC85B
201625	0.68	0.27	-1.332575339	0.000627809	Down	0.000112802	DNAH12
51021	93.9	37.41	-1.327701192	4.25E-68	Down	2.86E-70	MRPS16
427	9.96	3.97	-1.327006735	6.56E-11	Down	4.15E-12	ASAH1
2631	19.65	7.86	-1.321928095	1.37E-15	Down	5.67E-17	NIPSNAP2
4281	4.31	1.73	-1.316915831	5.48E-06	Down	6.62E-07	MID1
51170	12.95	5.2	-1.31636857	5.97E-07	Down	6.25E-08	HSD17B11
8360	482.15	194.44	-1.310157009	7.42E-62	Down	5.77E-64	HIST1H4D
79633	2.67	1.08	-1.30580843	1.73E-17	Down	6.25E-19	FAT4
55972	4.82	1.95	-1.305559022	3.30E-06	Down	3.86E-07	SLC25A40
1808	12.63	5.11	-1.305459443	1.11E-22	Down	2.96E-24	DPYSL2
7153	134.43	54.42	-1.304646271	2.84E-297	Down	1.40E-300	TOP2A
360023	7.54	3.06	-1.301032871	5.34E-22	Down	1.48E-23	ZBTB41
5567	5.48	2.23	-1.297132183	3.41E-09	Down	2.61E-10	PRKACB
84962	61.05	24.87	-1.295584788	5.16E-66	Down	3.59E-68	AJUBA
3489	142.39	58.16	-1.291748656	4.24E-50	Down	4.35E-52	IGFBP6
148213	3.94	1.61	-1.291134941	3.93E-10	Down	2.69E-11	ZNF681
3007	378.57	154.79	-1.290247817	7.95E-106	Down	2.75E-108	HIST1H1D
2044	2.22	0.91	-1.286621226	1.01E-06	Down	1.09E-07	EPHA5
51088	15.68	6.47	-1.277087942	3.63E-30	Down	6.99E-32	KLHL5

59345	30.14	12.44	-1.276692931	6.14E-69	Down	4.06E-71	GNB4
79624	13.06	5.43	-1.266130794	9.28E-13	Down	4.97E-14	ARMT1
56951	30.39	12.7	-1.258768178	3.18E-25	Down	7.50E-27	C5orf15
79699	20.22	8.46	-1.257053429	4.99E-44	Down	6.19E-46	ZYG11B
79948	5.66	2.37	-1.255914994	2.22E-05	Down	3.00E-06	PLPPR3
160418	19.54	8.21	-1.25097634	2.60E-44	Down	3.17E-46	TMTC3
3075	5.84	2.46	-1.247310054	3.47E-07	Down	3.49E-08	CFH
286148	7.95	3.36	-1.242493627	1.24E-17	Down	4.41E-19	DPY19L4
1977	31.25	13.21	-1.242225723	2.13E-37	Down	3.28E-39	EIF4E
23657	60.6	25.65	-1.240358968	2.06E-162	Down	3.57E-165	SLC7A11
5525	12.74	5.4	-1.238333965	2.28E-14	Down	1.05E-15	PPP2R5A
5575	4.67	1.98	-1.23792212	5.20E-05	Down	7.47E-06	PRKAR1B
25998	16.65	7.06	-1.237782089	8.37E-37	Down	1.31E-38	IBTK
50484	9.4	4.01	-1.22905852	2.03E-16	Down	7.84E-18	RRM2B
7059	11.01	4.7	-1.228081807	1.12E-12	Down	6.08E-14	THBS3
85012	16.06	6.87	-1.225089889	8.17E-07	Down	8.73E-08	TCEAL3
7915	12.81	5.48	-1.225022677	5.23E-23	Down	1.36E-24	ALDH5A1
29994	2.71	1.16	-1.224168046	6.56E-07	Down	6.93E-08	BAZ2B
4258	20.41	8.75	-1.22192126	1.12E-05	Down	1.42E-06	MGST2
8519	20.43	8.77	-1.220040456	1.59E-05	Down	2.09E-06	IFITM1
497661	13.19	5.67	-1.218023924	1.63E-08	Down	1.37E-09	C18orf32
54165	11.46	4.93	-1.216947492	1.40E-21	Down	3.93E-23	DCUN1D1
55204	11.11	4.79	-1.213761256	2.17E-12	Down	1.20E-13	GOLPH3L

55314	3.36	1.45	-1.212408333	0.00030695	Down	5.14E-05	TMEM144
55635	36.73	15.9	-1.207932131	2.47E-66	Down	1.71E-68	DEPDC1
100129543	8.54	3.7	-1.206710799	4.01E-08	Down	3.52E-09	ZNF730
51	21.2	9.19	-1.205927498	8.70E-54	Down	8.00E-56	ACOX1
83849	1.52	0.66	-1.203533394	6.58E-06	Down	8.09E-07	SYT15
6876	190.64	83.13	-1.19740974	6.55E-74	Down	3.84E-76	TAGLN
283431	16.18	7.07	-1.194429488	2.81E-19	Down	9.03E-21	GAS2L3
55088	2.56	1.12	-1.192645078	8.34E-06	Down	1.04E-06	CCDC186
55715	13.02	5.7	-1.191695624	6.51E-12	Down	3.77E-13	DOK4
149473	10.69	4.68	-1.191681418	0.000477631	Down	8.36E-05	CCDC24
4837	131.69	57.69	-1.190752629	9.54E-68	Down	6.48E-70	NNMT
5698	35.42	15.52	-1.190435655	2.44E-12	Down	1.36E-13	PSMB9
317	16.53	7.25	-1.189033824	3.53E-36	Down	5.70E-38	APAF1
6990	7.02	3.08	-1.18854068	1.12E-05	Down	1.42E-06	DYNLT3
25843	16.04	7.04	-1.188026808	4.08E-20	Down	1.25E-21	MOB4
3234	5.92	2.6	-1.187085553	5.91E-06	Down	7.19E-07	HOXD8
388591	7.42	3.26	-1.186547222	9.84E-10	Down	7.11E-11	RNF207
5764	10.59	4.66	-1.184300729	1.52E-05	Down	1.98E-06	PTN
51053	81.83	36.07	-1.181830429	2.76E-33	Down	4.80E-35	GMNN
3953	11.33	5	-1.180147861	2.21E-17	Down	8.02E-19	LEPR
60529	2.53	1.12	-1.175638653	4.37E-05	Down	6.20E-06	ALX4
6583	4.76	2.11	-1.173718575	0.000997338	Down	0.00018812	SLC22A4
115106	45.57	20.26	-1.169450196	1.08E-16	Down	4.11E-18	HAUS1

51084	8.25	3.67	-1.168614056	0.000212742	Down	3.45E-05	CRYL1
23129	10.51	4.7	-1.161030007	2.70E-12	Down	1.51E-13	PLXND1
81031	6.54	2.93	-1.158389971	2.35E-09	Down	1.77E-10	SLC2A10
64065	8.78	3.94	-1.15602531	2.39E-12	Down	1.33E-13	PERP
3400	3.32	1.49	-1.155870911	0.00011084	Down	1.70E-05	ID4
6091	17.93	8.05	-1.1553148	1.56E-41	Down	2.10E-43	ROBO1
54492	1.87	0.84	-1.154577037	0.000338235	Down	5.71E-05	NEURL1B
127933	28.38	12.77	-1.152116064	3.50E-76	Down	1.96E-78	UHMK1
135293	19.11	8.6	-1.151919213	1.07E-14	Down	4.83E-16	PM20D2
26973	38.64	17.41	-1.150178891	2.01E-40	Down	2.78E-42	CHORDC1
51144	32.94	14.85	-1.149377624	1.83E-23	Down	4.67E-25	HSD17B12
23306	24.22	10.92	-1.149226009	1.09E-47	Down	1.22E-49	NEMP1
2633	4.69	2.12	-1.145523658	3.51E-05	Down	4.91E-06	GBP1
6618	17.65	7.98	-1.145207532	6.36E-09	Down	5.07E-10	SNAPC2
116068	6.21	2.81	-1.144023138	3.78E-09	Down	2.91E-10	LYSMD3
54930	41.43	18.76	-1.143015992	8.85E-21	Down	2.62E-22	HAUS4
91752	4.08	1.85	-1.141043881	1.68E-06	Down	1.86E-07	ZNF804A
1468	36.2	16.42	-1.14053557	2.39E-22	Down	6.52E-24	SLC25A10
8790	9.68	4.4	-1.137503524	3.96E-14	Down	1.87E-15	FPGT
25978	14.43	6.58	-1.132911811	4.04E-12	Down	2.30E-13	CHMP2B
9768	98.03	44.71	-1.132625777	2.07E-44	Down	2.51E-46	PCLAF
23101	2.63	1.2	-1.132028394	2.47E-05	Down	3.35E-06	MCF2L2
388962	76.11	34.8	-1.128998714	3.41E-12	Down	1.93E-13	BOLA3

6492	3.87	1.77	-1.128584206	6.50E-08	Down	5.90E-09	SIM1
1182	17.4	7.96	-1.12824697	7.97E-21	Down	2.35E-22	CLCN3
64110	30.16	13.81	-1.126923109	1.11E-15	Down	4.58E-17	MAGEF1
26227	5.39	2.47	-1.125774231	0.000680151	Down	0.000123256	PHGDH
2332	9.95	4.56	-1.125662701	1.49E-13	Down	7.39E-15	FMR1
223082	4.8	2.2	-1.125530882	1.29E-05	Down	1.65E-06	ZNRF2
51196	2.94	1.35	-1.122856748	2.05E-06	Down	2.31E-07	PLCE1
130576	10.34	4.76	-1.119202707	1.77E-05	Down	2.35E-06	LYPD6B
51574	16.12	7.43	-1.117417628	6.95E-11	Down	4.42E-12	LARP7
728392	28.12	13.01	-1.111975632	9.76E-13	Down	5.24E-14	LOC728392
253982	11.65	5.39	-1.111972777	1.66E-05	Down	2.19E-06	ASPHD1
1353	31.76	14.75	-1.106495958	2.40E-14	Down	1.11E-15	COX11
151473	5.06	2.35	-1.106476628	1.23E-07	Down	1.16E-08	SLC16A14
6715	15.24	7.1	-1.101971973	3.43E-11	Down	2.12E-12	SRD5A1
5911	7.14	3.33	-1.100401897	1.57E-09	Down	1.17E-10	RAP2A
54507	4.93	2.3	-1.099953785	7.36E-08	Down	6.72E-09	ADAMTSL4
5292	23.68	11.07	-1.097013859	4.31E-19	Down	1.40E-20	PIM1
81537	40.42	18.92	-1.095157233	1.31E-39	Down	1.87E-41	SGPP1
5523	3.94	1.85	-1.090670359	1.41E-08	Down	1.18E-09	PPP2R3A
3714	4.51	2.12	-1.089063169	4.52E-08	Down	3.99E-09	JAG2
8908	9.46	4.45	-1.088034847	1.54E-09	Down	1.14E-10	GYG2
51435	10.2	4.8	-1.087462841	3.61E-10	Down	2.47E-11	SCARA3
874	21.75	10.24	-1.086799686	1.61E-07	Down	1.55E-08	CBR3

5825	46.61	21.95	-1.086418573	1.83E-35	Down	3.03E-37	ABCD3
55872	41.45	19.54	-1.084941634	5.41E-25	Down	1.29E-26	PBK
1386	22.41	10.57	-1.084167272	6.22E-23	Down	1.62E-24	ATF2
10681	14.64	6.91	-1.083157938	7.84E-14	Down	3.82E-15	GNB5
7008	4.65	2.2	-1.079727192	2.39E-06	Down	2.75E-07	TEF
30832	9.91	4.7	-1.076224301	1.16E-16	Down	4.44E-18	ZNF354C
23098	4.47	2.12	-1.076210567	1.09E-09	Down	7.91E-11	SARM1
2764	47.65	22.6	-1.076153441	2.14E-55	Down	1.86E-57	GMFB
114882	18.82	8.93	-1.075534548	1.58E-38	Down	2.35E-40	OSBPL8
65084	10.85	5.16	-1.072252072	2.66E-13	Down	1.36E-14	TMEM135
121274	10.74	5.11	-1.071598797	2.51E-14	Down	1.17E-15	ZNF641
221	22.67	10.8	-1.069753079	1.13E-18	Down	3.78E-20	ALDH3B1
6281	44.26	21.1	-1.068760452	3.10E-13	Down	1.59E-14	S100A10
9064	6.75	3.22	-1.067826814	1.23E-07	Down	1.16E-08	MAP3K6
55728	4.84	2.31	-1.067114196	4.32E-13	Down	2.26E-14	N4BP2
221079	11.39	5.44	-1.06608919	1.91E-25	Down	4.48E-27	ARL5B
4591	29.32	14.03	-1.063370095	9.81E-31	Down	1.85E-32	TRIM37
90488	41.13	19.72	-1.06053152	6.21E-39	Down	9.07E-41	TMEM263
134429	26.09	12.51	-1.060415155	8.34E-37	Down	1.31E-38	STARD4
23468	29.67	14.25	-1.058043008	1.02E-94	Down	4.20E-97	CBX5
55701	9.64	4.63	-1.058020953	1.98E-15	Down	8.35E-17	ARHGEF40
5962	57.26	27.51	-1.057571531	4.11E-84	Down	1.98E-86	RDX
8351	651.4	313.04	-1.057196704	6.50E-159	Down	1.16E-161	HIST1H3D

10278	4.6	2.22	-1.051074185	0.000125026	Down	1.94E-05	EFS
6738	33.55	16.22	-1.048538947	4.01E-92	Down	1.68E-94	TROVE2
4130	1.26	0.61	-1.046542586	0.000303832	Down	5.08E-05	MAP1A
57107	7.45	3.61	-1.045241588	1.85E-05	Down	2.47E-06	PDSS2
1033	239.07	115.89	-1.04467702	2.27E-52	Down	2.19E-54	CDKN3
57045	28.01	13.58	-1.044458504	1.52E-28	Down	3.12E-30	TWSG1
133418	12.31	5.97	-1.044027925	1.56E-14	Down	7.10E-16	EMB
92140	21.64	10.5	-1.043311171	1.16E-34	Down	1.98E-36	MTDH
128	52.88	25.7	-1.040953817	2.19E-37	Down	3.40E-39	ADH5
11187	28.74	14.02	-1.035573712	4.94E-22	Down	1.36E-23	PKP3
892	29.5	14.4	-1.034646143	8.16E-24	Down	2.03E-25	CCNC
149345	14.07	6.87	-1.034240324	1.34E-06	Down	1.46E-07	SHISA4
7846	135.73	66.31	-1.033441271	4.13E-68	Down	2.75E-70	TUBA1A
653464	21.94	10.72	-1.03325862	1.53E-25	Down	3.58E-27	SRGAP2C
85313	12.77	6.25	-1.03083043	5.69E-09	Down	4.47E-10	PPIL4
112817	7.64	3.74	-1.030534368	8.11E-06	Down	1.01E-06	HOGA1
9666	14.82	7.26	-1.029503994	1.10E-19	Down	3.43E-21	DZIP3
79144	20.47	10.03	-1.029189496	0.000104786	Down	1.59E-05	PPDPF
1633	17.75	8.7	-1.028731719	1.66E-12	Down	9.06E-14	DCK
199777	6.44	3.16	-1.02713613	3.32E-07	Down	3.34E-08	ZNF626
51122	13.17	6.47	-1.025417728	3.51E-13	Down	1.83E-14	COMMD2
55742	11.48	5.64	-1.025355574	2.89E-26	Down	6.57E-28	PARVA
5101	5.17	2.54	-1.025335784	7.43E-10	Down	5.28E-11	PCDH9

285605	4.92	2.42	-1.023651268	2.55E-08	Down	2.17E-09	DTWD2
8346	794.64	391	-1.023132809	2.36E-83	Down	1.18E-85	HIST1H2BI
23600	8.29	4.08	-1.02280295	7.22E-06	Down	8.92E-07	AMACR
6817	45.28	22.29	-1.022477342	4.35E-15	Down	1.88E-16	SULT1A1
4942	69.37	34.23	-1.019050592	9.09E-37	Down	1.44E-38	OAT
10513	17.45	8.62	-1.017467262	1.50E-29	Down	2.98E-31	APPBP2
201895	8	3.96	-1.01449957	1.57E-11	Down	9.37E-13	SMIM14
7289	23.58	11.68	-1.013523444	2.60E-21	Down	7.35E-23	TULP3
23564	70.34	34.86	-1.012772765	2.59E-23	Down	6.68E-25	DDAH2
65983	10.53	5.22	-1.012383724	1.25E-07	Down	1.18E-08	GRAMD3
6683	15.06	7.47	-1.011541622	1.03E-17	Down	3.66E-19	SPAST
348110	9.23	4.58	-1.01098305	2.71E-14	Down	1.26E-15	ARPIN
90806	12.57	6.24	-1.010366716	1.88E-15	Down	7.86E-17	ANGEL2
10810	5.11	2.54	-1.008494794	7.00E-07	Down	7.42E-08	WASF3
51315	11.99	5.97	-1.006028822	1.19E-05	Down	1.52E-06	KRCC1
135112	7.75	3.86	-1.005595463	6.64E-10	Down	4.68E-11	NCOA7
10447	13.3	6.63	-1.00434547	5.87E-09	Down	4.63E-10	FAM3C
91663	11.37	5.67	-1.003811614	7.96E-10	Down	5.67E-11	MYADM
23371	5.33	2.66	-1.002709287	4.63E-07	Down	4.74E-08	TNS2
10398	72.22	36.08	-1.001199082	3.42E-21	Down	9.72E-23	MYL9
54494	6.96	3.48	-1	0.000191913	Down	3.08E-05	C11orf71